

VOLCANICLASTIC SEDIMENT INPUT AND ENVIRONMENTAL RESPONSES OF FLUVIAL SYSTEMS: EXPLORING A CRETACEOUS EXAMPLE FROM PATAGONIA

Pablo Martín Villegas^{*1,2}, Aldo Martín Umazano^{1,2}

¹ INCITAP (Consejo Nacional de Investigaciones Científicas y Técnicas-Universidad Nacional de La Pampa), Rivadavia 234, 6300, Santa Rosa, Argentina.

² Facultad de Ciencias Exactas y Naturales, Universidad Nacional de La Pampa, Avenida Uruguay 151, 6300, Santa Rosa, La Pampa, Argentina.

*Corresponding author: pmvillegas90@gmail.com

ARTICLE INFO

Article history

Received May 4, 2023

Accepted September 9, 2023

Available online October 10, 2023

Handling Editor

José I. Cuitiño

Keywords

Fluvial responses

Aeolian processes

Volcaniclastic input

Tectonic activity

Climate change

Cretaceous

Patagonia

ABSTRACT

The input of large volumes of volcaniclastic sediments causes significant changes and imbalances in natural systems, with the consequent readjustment of depositional environments. In fluvial systems, this can affect the hydrogeomorphology, sedimentary processes (e.g., the development of aeolian processes), composition of detritus, soil features, and ecosystems. Consequently, some changes detected in the sedimentary record can be usually linked to volcaniclastic sediment supply, mainly in near vent positions. In this context, the analyzed Cretaceous stratigraphic interval of the Somuncurá-Cañadón Asfalto Basin (Argentina) in the Gorro Frigio depocenter, offers the possibility of testing the temporal evolution of a fluvial system in relation to changes in the influx of volcaniclastic material from a distant source. The goal of this contribution is to evaluate in detail the paleoenvironmental responses registered in the upper Bardas Coloradas and Puesto La Paloma members of the Los Adobes and Cerro Barcino formations, respectively, as well as to link these changes to all cyclical controls on sedimentation. Seven facies associations were defined including low sinuosity fluvial channel (FA1), meandering-like crevasse channel (FA2), crevasse splay (FA3), distal floodplain (FA4), aeolian (FA5), sheet-floods (FA6), and volcaniclastic channel (FA7). These FAs are arranged in three informal stratigraphic intervals: the lower stratigraphic interval A (upper Bardas Coloradas Member, 35 m thick) includes low sinuosity fluvial channels which transported a sandy bedload towards the NW, together with vegetated floodplain zones characterized by the presence of meandering-like crevasse channels, crevasse splays, and shallow lakes or ponded zones. The intermediate stratigraphic interval B (lower Puesto La Paloma Member, 11-16 m thick) records a volcaniclastic-rich aeolian system composed of 2D aeolian dunes that migrated towards SE and were spatially related to wet- and dry-interdune zones where the sedimentation mostly occurred from subaqueous and subaerial settling of suspended volcaniclastic sediments, respectively. The overlying stratigraphic interval C (upper Puesto La Paloma Member, 6-18 m thick) indicates volcaniclastic-rich fluvial sedimentation characterized by unconfined flows, which were sediment-laden or diluted, and showing lateral relationships with ponded areas. Locally, there was a volcaniclastic channel that transported

volcaniclastic gravels towards the NW. The assessment of allocyclic controls suggests that the variations in the volcaniclastic sediment supply were the main control governing the changes in the depositional systems. Consequently, the tectonic activity, eustatic sea-level modifications, basement morphology, and climatic changes would not have played an important role.

INTRODUCTION

The environmental responses detected in fluvial successions are directly or indirectly related to allocyclic factors including tectonic activity, climate change, and eustatic sea-level modifications (Miall, 1996, 2000, 2014; Bridge, 2003, 2006; Catuneanu *et al.*, 2009; Paredes, 2022). Many proxies can be used to establish the control of one or more of the mentioned factors, which should be evaluated together to obtain an integrated interpretation of the fluvial successions. The environmental modifications inferred from volcaniclastic-rich fluvial successions are classically linked with the temporal variation in the sediment supply from proximal to distal areas (Smith, 1991; Nakayama and Yoshikawa, 1997; Kataoka and Nakajo, 2002; Martina *et al.*, 2006; Sierra *et al.*, 2009; Umazano *et al.*, 2012, 2017; Cuitiño and Scasso, 2013; Sohn *et al.*, 2013; Raigemborn *et al.*, 2015, 2018; Spalletti and Colombo Piñol, 2019; Di Capua and Scasso, 2020; Kataoka, 2023). In this type of fluvial environments, the disturbances produced by volcaniclastic sediment influx include complex changes in hydrogeomorphology, sedimentation, composition of detritus, soil features, and ecosystems (Manville *et al.*, 2009; Pierson and Major, 2014; Petrinovic and D'Elía, 2018; Critelli *et al.*, 2023). These changes are frequently sudden and repetitive, originating cyclic sedimentation patterns during alternating syn- and inter-eruptive conditions (*sensu* Smith, 1991). However, the resulting successions are less foreseeable because other controlling factors also have a significant influence on sedimentary paleoenvironments (Umazano *et al.*, 2022; Villegas, 2022; Paredes, 2023). In fact, several papers explored other controlling factors to obtain consistent explanations, including valuation of tectonic activity (Umazano *et al.*, 2012; Sohn *et al.*, 2013; Paredes *et al.*, 2015; Carmona *et al.*, 2016; Monti and Franzese, 2016; Umazano *et al.*, 2017; Villegas *et al.*, 2019; D'Elía *et al.*, 2020), climate change (Umazano *et al.*, 2008, 2017; Raigemborn *et al.*, 2018; Paredes

et al., 2018, 2020; D'Elía *et al.*, 2020), basement morphology (Allard *et al.*, 2014; Foix *et al.*, 2020) and development of complex hydrometeorological phenomena (Umazano *et al.*, 2014, Umazano y Melchor, 2020; Umazano *et al.*, 2022).

Aeolian dunes are also relatively common components in volcaniclastic fluvial environments both in proximal and distal sectors (White, 1989, 1990; Smith and Katzman, 1991; Umazano *et al.*, 2014, 2017). These landforms are frequently formed after resedimentation or reworking of primary volcanic products mainly in semiarid to arid climatic conditions (Edgett and Lancaster, 1993). Nevertheless, aeolian dune deposits have also been documented in humid environments suggesting they should be used with caution for paleoclimatic inferences (Umazano *et al.*, 2014).

In this context, the present contribution documents and analyses fluvial and aeolian processes from a Cretaceous endorheic, volcaniclastic-rich fluvial succession in an extra-Andean Patagonian basin. Particularly, we analyse the Bardas Coloradas and Puesto La Paloma members in the Gorro Frigio depocenter (Chubut province; Fig. 1). The aim of this paper is to examine the response of this fluvial-aeolian succession to the volcaniclastic influx from a distal source, together with the climate change and intrabasinal tectonic activity.

SOMUNCURÁ-CAÑADÓN ASFALTO BASIN

The Somuncurá-Cañadón Asfalto Basin, located in Argentinian extra-andean Patagonia (Fig. 1), developed since the Jurassic in relation with the Gondwana breakup and opening of the South Atlantic Ocean (Cortiñas, 1996; Uliana and Biddle, 1987; Figari *et al.*, 2015; Giacosa, 2020, Figari and Hechem, 2022). Its basement includes Paleozoic-Triassic igneous and metamorphic rocks named Lipetrén, Mamil Choique and Cushamen formations (Allard *et al.*, 2022; Lagorio *et al.*, 2022; Fig. 2). The overlying Jurassic-Cretaceous infilling is divided in

three megasequences, which are limited by regional unconformities, named in chronological order as J1, J2, and K (Figari *et al.*, 2015; Fig. 2). The lower two megasequences were deposited during Early Jurassic-Early Cretaceous rift conditions: 1) the Las Leoneras Formation, which is a fluvial-lacustrine succession cropping out in the western sector of the basin (Nakayama, 1973; Pol *et al.*, 2011); 2) the widely distributed volcanic rocks with sedimentary

intercalations included in the Lonco Trapial/Marifil formations (Lesta and Ferello, 1972; Hauser *et al.*, 2017); and 3) the alluvial to lacustrine sedimentary successions deposited in several troughs in the western part of the basin recorded in the Cañadón Asfalto and Cañadón Calcáreo formations (Stipanovic *et al.*, 1968; Proserpio, 1987; Volkheimer *et al.*, 2009; Cúneo *et al.*, 2013).

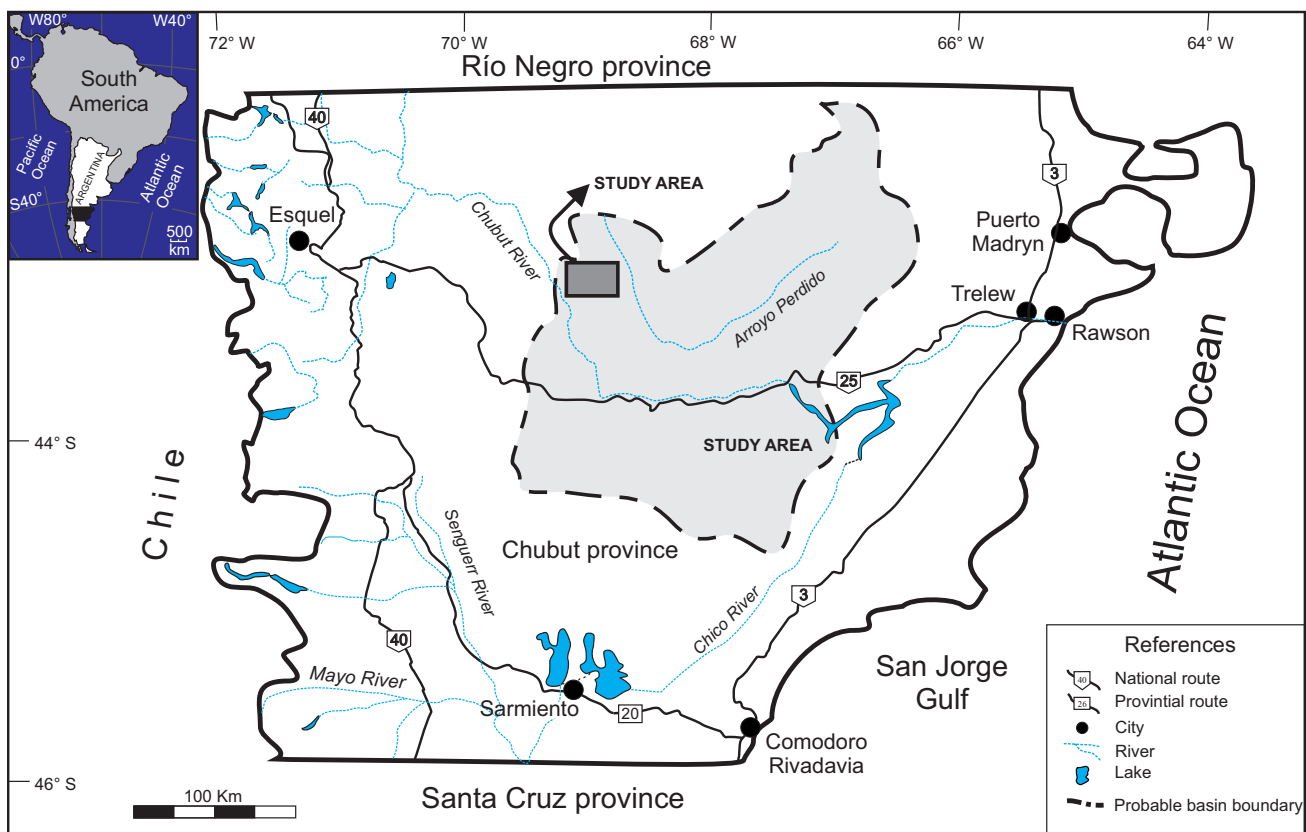


Figure 1. Location map of the Somuncurá-Cañadón Asfalto Basin in extra-andean Patagonia (light grey area, after Umazano *et al.*, 2017). Study area (dark grey rectangle) corresponds to Figure 3.

After an episode of extensional reactivation, the Early Cretaceous-Paleogene megasequence K was deposited (Fig. 2), initially during the tectonic reactivation stage and later during sag conditions leading to a wider depositional area (Figari *et al.*, 2015). In turn, the basal discordance of the megasequence K has been recently related to basin-scale compressive deformation (Allard *et al.*, 2022), or even with a “mid” Cretaceous compressive tectonic setting associated with the generation of the Patagonian broken foreland that extends beyond the basin boundaries (Gianni *et al.*, 2015; Echaurren *et al.*, 2016; Butler *et al.*, 2020;

Gianni *et al.*, 2022). The megasequence K includes the Chubut Group, composed of the Los Adobes and Cerro Barcino formations (*sensu* Codignotto *et al.*, 1978; Fig. 2). The Los Adobes Formation is composed of an alluvial siliciclastic, coarse-grained succession named Arroyo del Pajarito Member (Codignotto *et al.*, 1978). This is overlain by the Bardas Coloradas Member, dominated by sandstones and mudstones with scarce volcaniclastic strata, deposited by different types of rivers and vegetated floodplains (Allard *et al.*, 2009, 2010a, 2010b, 2011, 2012; Villegas *et al.*, 2014; Brea *et al.*, 2016; De Sosa Tomas *et al.*, 2021).

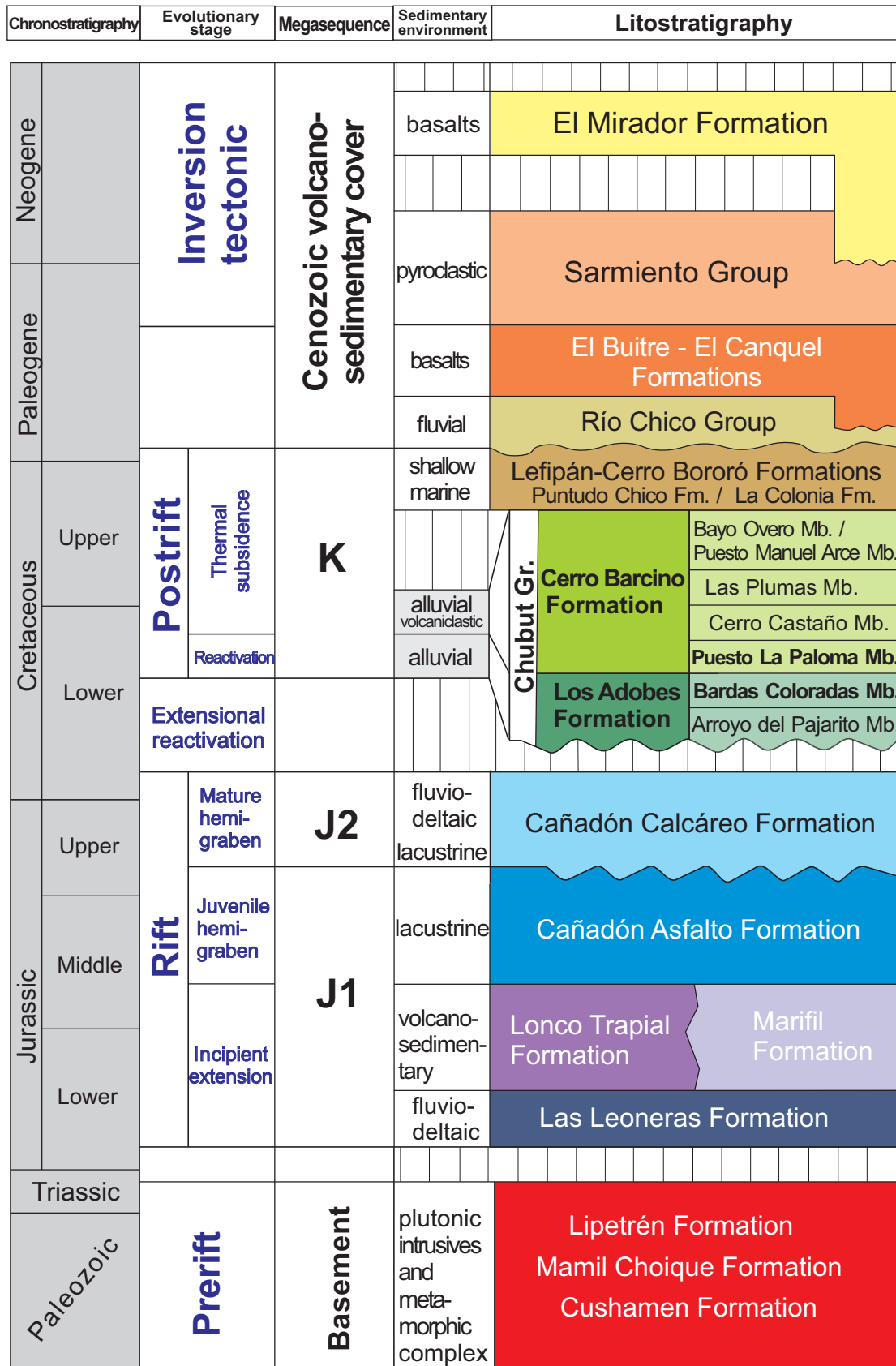


Figure 2. Stratigraphy of the Somuncurá-Cañadón Asfalto Basin (modified from Villegas, 2022). Evolutionary stages and megasequences from Figari *et al.* (2015).

The overlying Cerro Barcino Formation initiates with the Puesto La Paloma Member, which is mainly composed of sheet-like volcaniclastic strata mostly deposited in unconfined fluvial conditions and in some aeolian and lacustrine environments (de la Fuente *et al.*, 2011; Villegas *et al.*, 2014; Sterli *et al.*, 2015; Brea *et al.*, 2016; De Sosa Tomas *et al.*, 2017; Umazano *et al.*, 2017; Krause *et al.*, 2020; Melchor *et al.*, 2023). This member is overlain by a sandstone-dominated succession showing channel-like bodies, interbedded with finer-grained sheet-like volcaniclastic strata, accumulated in channelled fluvial systems. These are named in ascending stratigraphic order: Cerro Castaño Member, Las Plumas Member, and Bayo Overo-Puesto Manuel Arce members (e.g., Codignotto *et al.*, 1978; Manassero *et al.*, 2000; Cladera *et al.*, 2004; Genise *et al.*, 2010; Foix *et al.*, 2012; Carmona *et al.*, 2016; Umazano *et al.*, 2017; Krause *et al.*, 2020; Villegas, 2022). The Las Plumas Member records alluvial fan sedimentation in the eastern margin of the basin linked with syn-sedimentary normal faults (Allard *et al.*, 2014; Villegas *et al.*, 2019; Villegas, 2022). The megasequence K culminates with the deposition of Atlantic, shallow marine and associated coastal to

continental sediments, referred as to the Puntudo Chico, La Colonia, Lefipán - Cerro Bororó formations, and lateral equivalents (Fig. 2).

STUDY AREA

The Gorro Frigio depocenter is a half-graben with an inverted master fault in its western boundary (Figari *et al.*, 2015; Fig. 3). The master fault mostly exhibits a NNW-SSE orientation, which is roughly parallel to the Chubut River, and vergence towards the NE. However, the orientation of the master fault is NE-SW in the northern and southern boundaries of the structure, where the vergences are towards the SE and NW respectively (Fig. 3). There is a lower hierarchy inverted fault in the southern part of the half-graben, which is roughly parallel to the master fault and has similar vergence, giving rise to a compartmentalized sub-basin. Moreover, there are several secondary faults in the study area, showing both normal and strike displacements with different trends, and multiscale folding with variable orientation of the axial traces and occasional plunge (Fig. 3). In evolutionary terms, the depocenter had an initial syn-rift phase, followed by contractional

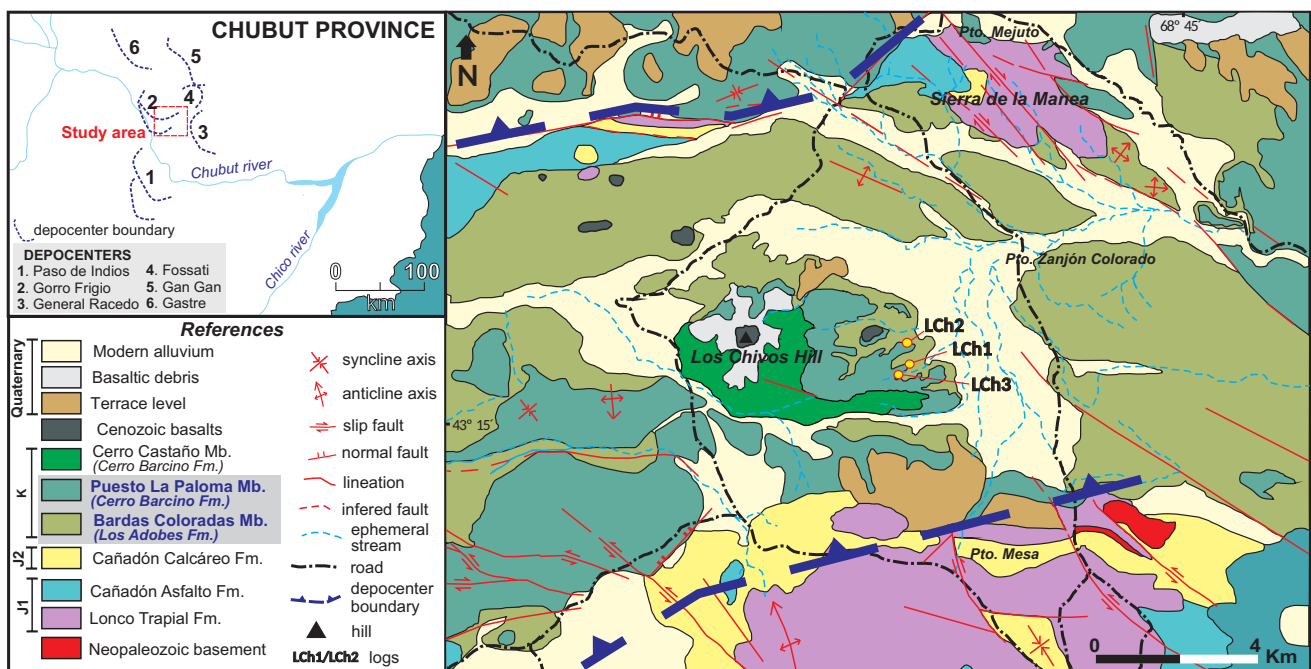


Figure 3. Geological map of the Los Chivos hill and surrounding area. The position of the measured sections is indicated. The location of the depocenters is modified from Figari *et al.* (2015).

processes that inverted the master fault, folded the sedimentary record of the megasequences J1 and J2, and generated an unconformity surface. Then, the deposition of the Megasequence K occurred in renewed extensional conditions that produced asymmetric subsidence of the basement. Finally, the whole sequence was deformed during the compression associated with the Cenozoic tectonic inversion (Allard *et al.*, 2022).

The study area corresponds to the southern sector of the Gorro Frigio depocenter, where Los Chivos hill is one of the most notable physiographic elements (Figs. 3-4). In the study area, there are isolated outcrops of megasequences J1 and J2, including volcanic rocks of the Lonco Trapial Formation and sedimentary

successions of the Cañadón Asfalto and Cañadón Calcáreo formations (Proserpio, 1987; Umazano *et al.*, 2017; Krause *et al.*, 2020). The Megasequence K is widely exposed in the area (Fig. 3). It is represented mainly by the Bardas Coloradas Member of the Los Adobes Formation, which is covered in transitional contact by the Puesto La Paloma and Cerro Castaño members (Fig. 4) of the Cerro Barcino Formation. According to U/Pb zircon dates of tuffaceous strata and field relationships, the Bardas Coloradas and Puesto La Paloma members are assigned Barremian-Aptian and Aptian ages, respectively (Krause *et al.*, 2020). These rocks are intruded by a volcanic neck (Fig. 4) and several dikes (Proserpio, 1987).

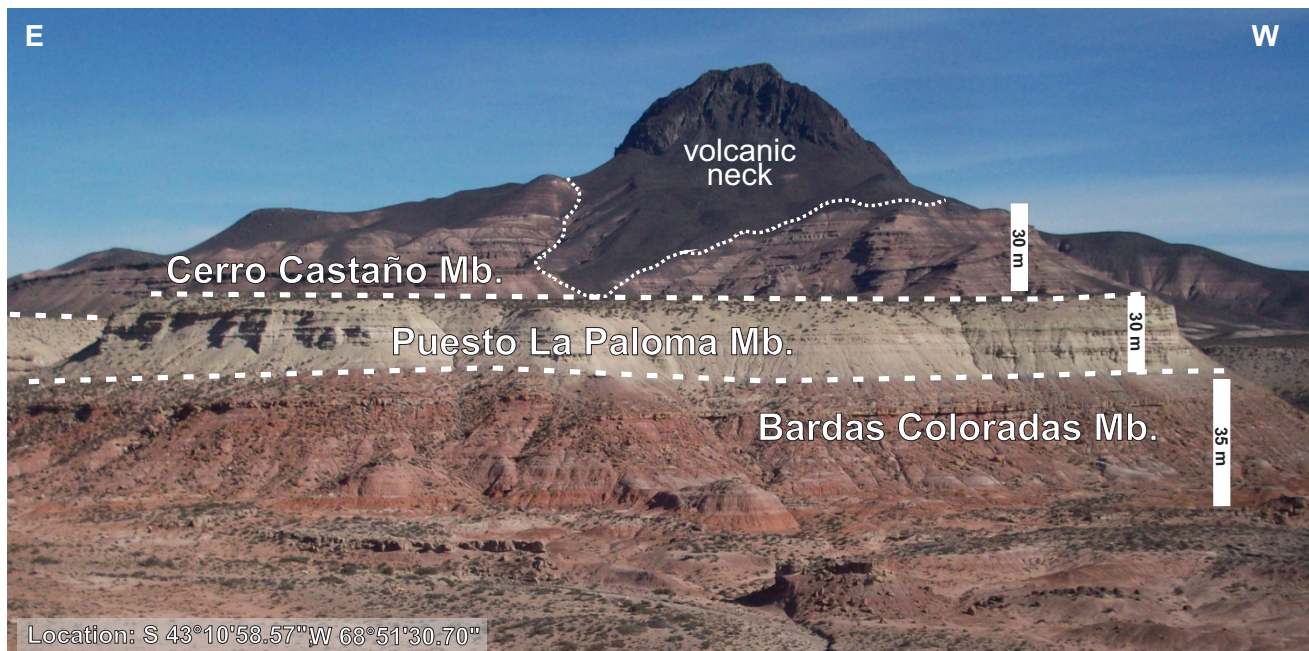


Figure 4. View looking southward of the Los Chivos hill, where the Bardas Coloradas, Puesto La Paloma, and Cerro Castaño members of the Chubut Group crops out.

In this contribution, we analyse the sedimentary record of the Cretaceous Bardas Coloradas and Puesto La Paloma members, which would have been deposited under relatively similar semiarid-arid climatic conditions (*e.g.*, Krause *et al.*, 2014; Allard *et al.*, 2022). We investigated those units in three sites named Los Chivos 1, Los Chivos 2, and Los Chivos 3 (hereafter referred as to LCh1, LCh2, and LCh3, respectively) (Fig. 3). All logs include partial sections of the Bardas Coloradas Member, which is an up to ~35 m thick succession (Fig. 4) mostly composed of sandstone and/or sandstone-conglomeratic bodies

with channel-like geometry interbedded with finer-grained tabular strata of mudstones, sandstones, and subordinated volcanoclastic-rich sandstones (Figs. 4 and 5). LCh3 log includes the complete section of Puesto La Paloma Member, whereas in the remaining sites the upper part of the unit is not exposed (Fig. 5). The Puesto La Paloma Member is an up to ~30 m thick succession (Fig. 4) mainly composed of sheet-like strata of volcanoclastic sandstones and tuffs with subordinated participation of volcanoclastic-rich mudstones and breccias (Figs. 4 and 5).

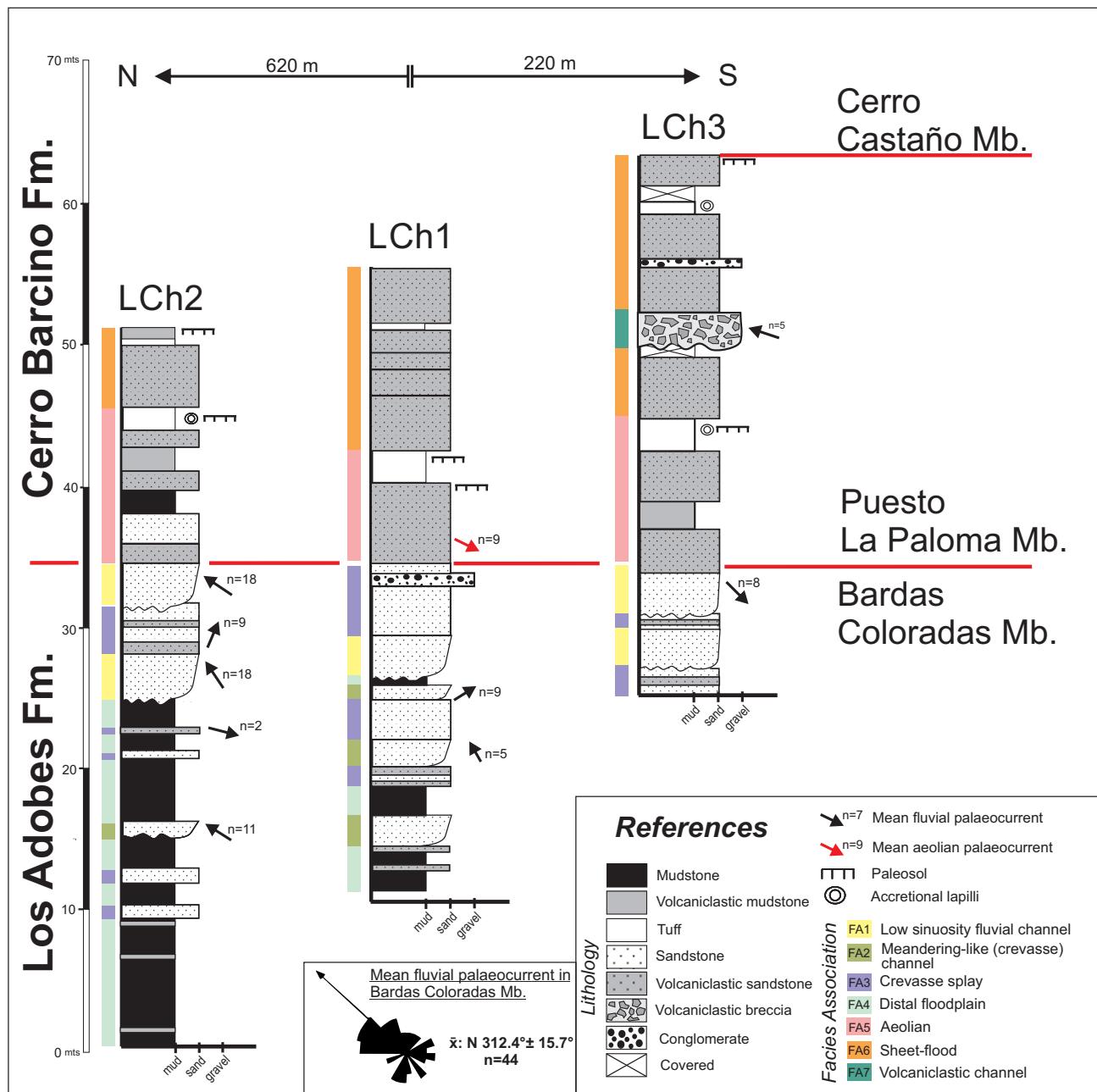


Figure 5. Correlation of sedimentary logs of the Bardas Coloradas and Puesto La Paloma members showing the recognized facies associations (colour bars to the left of the logs) and paleocurrent directions of fluvial and aeolian deposits.

METHODS AND TERMINOLOGY

Basic attributes considered during the measurement of detailed sedimentological sections were lithology, grain-size, sorting, sedimentary structures, paleocurrents, and fossil content. The primary volcaniclastic rocks are termed tuff, whereas the volcaniclastic adjective emphasizes the secondary origin of breccias, sandstones, and mudstones.

Sedimentary facies were described according to the criteria of Miall (1978) but applied to volcaniclastic fluvial successions with aeolian influence (Umazano *et al.*, 2017). Specifically, an additional symbol (*) was employed to highlight the well sorting of the deposits. The geometry of sedimentary bodies is defined by width (W), length (L), and thickness (T) parameters *sensu* Bridge (1993). When both margins of channelled deposits were exposed, the true width of these fluvial bodies

was obtained from apparent measurements corrected by the mean paleocurrent (*e.g.*, Paredes *et al.*, 2007; Umazano *et al.*, 2012). The minimum and maximum true width values were estimated by the empirical formulas of Bridge and Mackey (1993) and Bridge and Tye (2000), which are based on thickness of cross-bedded sets. Bounding surfaces were ranked according to Allen (1983), therefore the term strataset refers to stratigraphic intervals limited by second order surfaces (Umazano *et al.*, 2017). Third order surfaces limit groups of stratasets and commonly constitutes base and top of channelled bodies.

The architecture of the studied deposits was determined from direct measurement, tracing of key stratal surfaces on photomosaics, and the preparation of virtual outcrop models, which were made with georeferenced photographs acquired by drone flights. Aerial photographs of the outcrop were taken using

a Phantom 3 Pro (DJI, China) over several flights. To analyse the multi-scale sedimentary architecture of the succession, Structure-from-Motion (SfM) photogrammetry methods were used to generate three-dimensional (3D) virtual outcrops (Westoby *et al.*, 2012). Metashape© (Agisoft LLC) was used to generate photogrammetric virtual outcrop models.

FACIES ASSOCIATIONS

Twenty-one sedimentary facies were recognized (Table 1), which have been grouped in the following seven facies associations (FA): low sinuosity fluvial channel deposits (FA1), meandering-like crevasse channel deposits (FA2), crevasse splay deposits (FA3), distal floodplain deposits (FA4), aeolian deposits (FA5), sheet-flood deposits (FA6), and volcanoclastic channel deposits (FA7) (Table 2). The

Facies	Lithology and texture	Sedimentary structures	Fossil content	Interpretation
Cmm	Poorly-sorted, matrix-supported conglomerate	Massive	-	Debris-flow
Ch	Moderately well-sorted, clast-supported conglomerate, rare clast imbrication	Diffuse horizontal stratification	-	Fluvial channel lag
Cp	Moderately well-sorted, clast-supported conglomerate	Planar cross-bedding	-	Migration of gravel 2D dunes
Sp	Moderately well-sorted, coarse to fine-grained sandstone	Planar cross-bedding	Burrows	Sub-aqueous migration of sand 2D dunes; bioturbation
St	Moderately well-sorted, coarse to fine-grained sandstone	Trough cross-bedding, rare concretions	Burrows and root traces	Sub-aqueous migration of sand 3D dunes; bioturbation and pedogenesis
Sm	Moderately well-sorted, coarse to fine-grained sandstone	Massive, rare concretions	Root traces	Sediment (sand)-laden flow; pedogenesis
Sh	Moderately well-sorted, medium to fine-grained sandstone	Plane parallel lamination, rare desiccation cracks	-	Plane-bed conditions during streamflow; sub-aerial exposure of deposits
Mh	Mudstone	Plane parallel lamination or massive	Burrows and root traces	Settling of suspended sediments in standing water; bioturbation and pedogenesis
Mr	Mudstone	Ripples	-	Sub-aqueous migration of muddy ripples
VCmm	Very poorly-sorted, matrix-supported volcanoclastic conglomerate	Massive	-	Reworking of volcanoclastic substrates by debris-flow
VCt	Moderately well-sorted, clast-supported volcanoclastic conglomerate	Trough cross-bedding	-	Reworking of volcanoclastic substrates by sub-aqueous migration of gravel 3D dunes

VSp	Moderately well-sorted, fine-grained volcaniclastic sandstone	Planar cross-bedding	-	Reworking of volcaniclastic substrates by sub-aqueous migration of 2D dunes
VSp*	Well-sorted, fine-grained volcaniclastic sandstone	Planar cross-bedding, normal and reverse intralamina grading, rare concretions	Root traces	Migration of aeolian 2D dunes by grain-fall and grain-flow processes; pedogenesis
VSt	Moderately well-sorted, medium to fine-grained volcaniclastic sandstone	Trough cross-bedding, rare concretions	Burrows	Reworking of volcaniclastic substrates by water flows with development of 3D dunes; bioturbation
VSt*	Well-sorted, medium to fine-grained volcaniclastic sandstone	Trough cross-bedding, rare concretions	Burrows	Aeolian reworking of volcaniclastic substrates with development of 3D dunes; bioturbation
VSm	Moderately well-sorted, medium to fine-grained volcaniclastic sandstone	Massive, rare concretions	Burrows, root traces and transported logs	Reworking of volcaniclastic substrates by dilute flows with low water-sediment ratio; bioturbation and pedogenesis
VSh	Moderately well-sorted, medium to fine-grained volcaniclastic sandstone	Plane parallel lamination	Burrows and root traces	Reworking of volcaniclastic substrates by stream flows with development of plane beds; bioturbation and pedogenesis
VSr	Moderately well-sorted, medium to fine-grained volcaniclastic sandstone	Asymmetrical ripples	-	Reworking of volcaniclastic substrates by low energy currents with development of sand ripples
VMh	Volcaniclastic siltstone	Massive or horizontal lamination, rare concretions	Burrows and turtle remains	Settling of suspended volcaniclastic sediments in standing water; bioturbation
Tm	Well-sorted, fine-grained vitric tuff	Massive, levels with accretionary lapilli	Burrows and root traces	Subaerial ash-fall event in steady conditions; bioturbation and pedogenesis
Th	Well-sorted, fine-grained vitric tuff	Plane parallel lamination, levels with accretionary lapilli	Burrows and root traces	Discontinuous subaerial settling of volcanic ash; bioturbation and pedogenesis

Table 1. Description and interpretation of the sedimentary facies for the Bardas Coloradas and Puesto La Paloma members. Dark grey rows are epiclastic facies; light grey rows are reworked volcaniclastic facies; white rows are primary volcaniclastic facies. See explanation about the nomenclature in the text.

stratigraphic position of each facies association for every sedimentary log is shown in Figure 5. Field examples of facies associations are shown in figures 6 to 10.

Low sinuosity fluvial channel deposits (FA1)

FA1 includes multistory sandstone bodies with sheet to channel shapes, which commonly exhibit a fining-upward trend. Each body has erosive and concave-up to irregular base, whereas the top is usually flat. The thickness of individual FA1 deposits ranges from 2.6 to 3.4 m ($\bar{x} = 2.99$ m; $\sigma = 0.31$ m; $n=5$), the minimum true width varies from 121.5 to 246 m

($\bar{x} = 173.8$ m; $\sigma = 52$ m; $n=4$); and the maximum true width ranges from 329 to 562 m ($\bar{x} = 429.5$ m; $\sigma = 97.1$ m; $n=4$) (Table 3). Typically, the bodies comprise stratatasets of coarse to fine-grained sandstones with trough cross-bedding (facies St) and/or tabular planar cross-bedding (facies Sp) (Figs. 6a, b). There are centimeter- to decimeter-thick intercalations of massive matrix-supported conglomerates (facies Cmm) or sandstones with plane parallel lamination (facies Sh) or massive aspect (facies Sm). The lower part of the bodies commonly bears scarce gravel-size extra-clasts of volcanic nature, whereas the upper part of some bodies has burrows and root traces. In views oblique to the mean paleoflow, the second and

third order surfaces are essentially parallel to each other showing a near horizontal bedding. The dip directions of strataset tops and paleoflow data have similar directions (Fig. 7). Mean paleocurrent of individual bodies inferred from facies St suggests a general drainage towards NW and locally towards SE (Fig. 5).

Interpretation. FA1 is envisaged as low sinuosity fluvial channel deposits considering the parallel direction in the second order surfaces in views oblique to the mean paleocurrent data, which have similar trends from adjacent stratasets. The similarity between dip directions of strataset tops and associated cross-bedded sandstones, and the presence of erosive bases and fining-upward fill support this interpretation (Best and Bristow, 1993; Bridge *et al.*, 2000; Georgieff and González Bonorino, 2002; Bridge and Lunt, 2006; Umazano *et al.*, 2008, 2012; Paredes, 2022). Deposition mainly occurred by migration of sandy three and two-dimensional dunes, which are registered as facies St and Sp, respectively. The rare presence of massive and laminated sandstone strata (facies Sm and Sh) indicates the occasional occurrence of sediment (sand)-laden flows and plane-bed conditions. The remaining facies Cmm, which is massive and matrix supported, represents deposition from debris-flows; the reduced thickness of resulting deposits is probably a consequence of the common reworking of this type of deposits within fluvial channels. The rivers are considered to be perennial due to absence of evidence of subaerial exposure in the lower part of the bodies (Bridge *et al.*, 2000; Bridge 2003, 2006, Melchor *et al.*, 2012). In fact, the occasional burrows and root traces in the uppermost part of FA1 deposits represent biological activity after channel abandonment (Umazano *et al.*, 2017).

Meandering-like crevasse channel deposits (FA2)

FA2 comprises sandstone-dominated bodies with the following general features: i) channel and/or ribbon geometry; ii) erosive and irregular base, with concave-up morphology locally; iii) flat to undulated top; and iv) subtle upward decrease of grain-size. The thickness of individual FA2 deposits ranges from 1 to 1.8 m ($\bar{x} = 1.34$ m; $\sigma = 0.35$ m; $n=5$) and true width ranges from 13.9 m

to 51.2 m ($\bar{x} = 31.6$ m; $\sigma = 14.4$ m; $n=5$) (Table 3). Typical FA2 deposits show cross-bedded, coarse to fine-grained sandstones including St and Sp (Fig. 6c). The cross-bedded strata have tabular to lenticular intercalations up to ~1 m thick of laminated or massive sandstones (facies Sh and Sm, respectively), as well as conglomerates with horizontal stratification (facies Ch) or massive and matrix-supported features (facies Cmm). The presence of burrows and root traces is noted in some cross-bedded sandstones bodies, however, only in one case the root traces are in the lower part of a body. Architecturally, there are stratasets whose upper surfaces roughly dip both in the same direction and at high-angle in relation to the paleoflow data of associated cross-bedded sandstones (Fig. 8). Moreover, in views oblique to mean paleocurrent, they define a laterally stacked pattern (Fig. 8). Mean paleocurrent data of individual bodies measured from cross-bedded facies indicates a highly variable flow in a range between NW to NE (Fig. 5).

Interpretation. FA2 is considered as meandering-like fluvial channel deposits because the bodies with channel or ribbon geometry, erosive base and fining-upward trend include stratasets bounded by surfaces produced by lateral migration of point bars (Georgieff and Gonzalez Bonorino, 2002; Pérez *et al.*, 2013a; Umazano *et al.*, 2017; Paredes, 2022). The FA2 bodies are interpreted as crevasse channels because they are smaller than those of FA1, fine-grained, and show dissimilar mean paleocurrent orientations (Platt and Keller, 1992; Galloway and Hobday, 1996; Bristow *et al.*, 1999; Bridge *et al.*, 2000). In these channels, the sedimentation was dominated by migration of three and two-dimensional sand dunes recorded as facies St and Sp, respectively. Besides, there was episodic deposition of sands in plane bed conditions (facies Sh) and sediment-laden flows (facies Sm), as well as sedimentation of gravels from high energy currents (facies Ch) and debris-flows (facies Cmm). The root traces located in the lower part of the bodies indicate significant variability in water discharge up to a transient cessation of flow (Melchor *et al.*, 2012; Umazano *et al.*, 2014), which is typical of crevasse channels (Paredes, 2022).

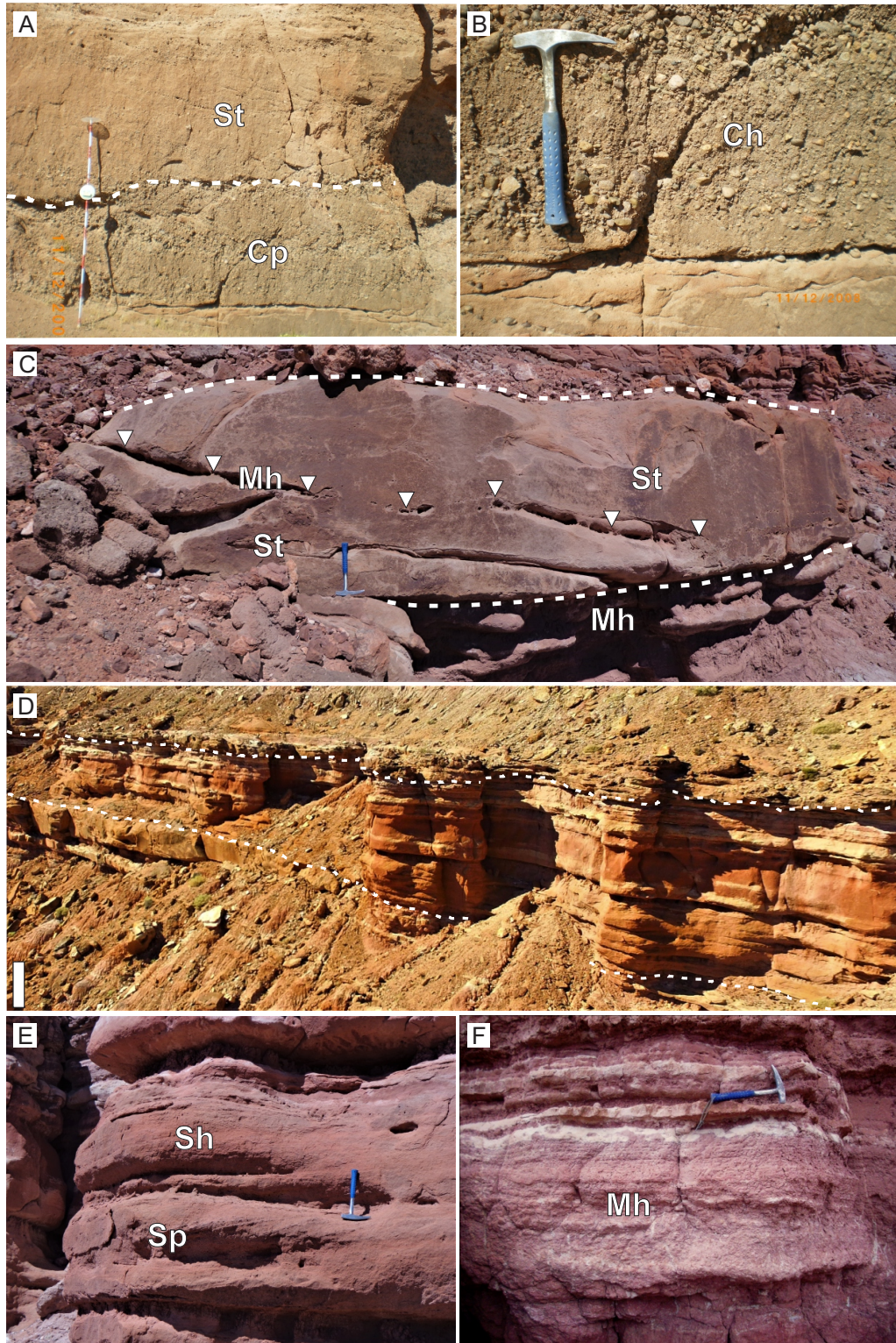


Figure 6. Examples of facies associations recognized in the Bardas Coloradas Member. **a)** Typical infill of FA1 deposits composed of sandstones with trough cross-bedding (facies St) and conglomerates with planar cross-bedding (facies Sp). Jacob staff is 1.5 m long. **b)** Contact between the cross-bedded sandstone facies mentioned in **a)** and a conglomerate with horizontal stratification (facies Ch). **c)** Body with channel-like geometry composed of trough cross-bedded sandstones (facies St) and finer grained sediments in lateral accretion surfaces indicated using white triangles (FA2). Base and top are marked with dashed lines. **d)** Panoramic view of a sheet-like body composed of sandstones with horizontal lamination (facies Sh), cross-bedding (facies St), and massive aspect (facies Sm) (FA3). Scale bar is 2 m long. **e)** Detail of cross-bedded and laminated sandstones (facies St and Sh) mentioned in **d)**. **f)** Laminated mudstones (facies Mh) from distal floodplain strata (FA4). In **b)**, **c)**, **e)** and **f)** hammer is 0.33 m long.

Crevasse splay deposits (FA3)

FA3 is characterized by sandstone bodies with occasional fining-upward trend and different morphologies including sheet-like and subtle plano-convex. Their bases are commonly slightly erosive. Sandstone bodies are commonly vertically stacked and/or laterally amalgamated, originating architecturally complex successions up to ~5 m thick and laterally continuous for up to several hundreds of meters. The dominant facies are medium to fine-grained sandstones with plane parallel lamination (Sh) and rare presence of desiccation cracks or massive features (Sm). The occurrence of rhythmic stratigraphic intervals, showing facies Sm and Sh, is common in the lower and upper part, respectively, which are typically separated by a transitional contact (Fig. 6d, e). In addition, there are rare occurrences of trough cross-bedded sandstones (St), massive and matrix-supported conglomerates (Cmm), and medium to fine-grained volcanoclastic facies which can be massive (VSm), laminated (VSh), or trough cross-bedded (VSt) sandstones. Paleocurrent data measured from cross-bedded facies indicate a mean flow direction towards NNE and SE. Burrows, root traces and other undifferentiated trace fossils are relatively common in sandstone and volcanoclastic sandstone facies.

Interpretation. FA3 is interpreted as crevasse splay deposits according to the recognized geometries and facies, as well as to the slightly erosive base of the bodies (Miall, 1996; Bristow *et al.*, 1999; Bridge *et al.*, 2000; Bridge and Demicco, 2008; Umazano *et al.*, 2008; Burns *et al.*, 2017; Paredes, 2022). Sediment was transported by different types of flows including debris-flows (facies Cmm), dilute flows with low water-sediment ratio that prevented the generation/preservation of bedforms (facies Sm and VSm), and diluted flows in which three-dimensional dunes (facies St and VSt) or plane bed conditions (Sh and VSh) were developed. The common vertical alternation between massive and laminated strata suggests that the dilution phenomenon (*sensu* Fisher, 1983) by water incorporation or sedimentation was recurrent. Deposits experienced subaerial exposure evidenced by the presence of desiccation cracks and root traces.

Distal floodplain deposits (FA4)

FA4 is represented by sheet bodies, with nonerosive bases, mainly composed of mudstones with plane parallel lamination (Mh) or massive (facies Mh) (Fig. 6f). The bodies are up to 20 m thick and show a lateral extension up to several hundreds of meters. They have scarce thin intercalations of massive, medium to fine-grained sandstones or volcanoclastic sandstones (facies Sm and VSm, respectively), mudstones with ripple cross-lamination (facies Mr) and laminated volcanoclastic mudstones (facies VMh). Very scarce bioturbation is present in mudstone facies including burrows and root traces.

Interpretation. FA4 suggests a distal floodplain environment where sedimentation was mostly dominated by settling of suspended fine-grained sediments in standing waters (Nanson and Croke, 1992; Umazano *et al.*, 2008, 2014, 2017; Paredes, 2022). Compositionally, the suspended sediments were mostly epiclastic and very rarely volcanoclastic-rich which are represented in facies Mh and VMh, respectively. The scarce intercalations of mudstone and sandstone facies indicate episodic sedimentation from current flows including migration of silty ripples (facies Mr), and sediment-laden flows with and without significant participation of volcanoclastic content (facies Sm and VSm, respectively).

Aeolian deposits (FA5)

FA5 comprises three sub-facies associations named FA5a, FA5b, and FA5c. FA5a includes bodies up to ~5 m thick and laterally continuous for more than 100 m, with plane-convex to sheet geometry (Fig. 9a), composed of very well-sorted, medium to fine-grained volcanoclastic sandstones with tabular planar cross-bedding (facies VSp*) and trough cross-bedding (facies VSt*) (Fig. 9b). Cross-bedded sets of VSp* facies have decimeter to meter thick foresets with dip angles up to 25° and exhibit both normal and intralamina reverse grading, as well as scarce root traces. Mean paleocurrent data of individual bodies measured from facies VSp* suggests a main wind direction towards the SE. FA5b contains bodies with mantle bedding and non-erosive bases composed of fine-

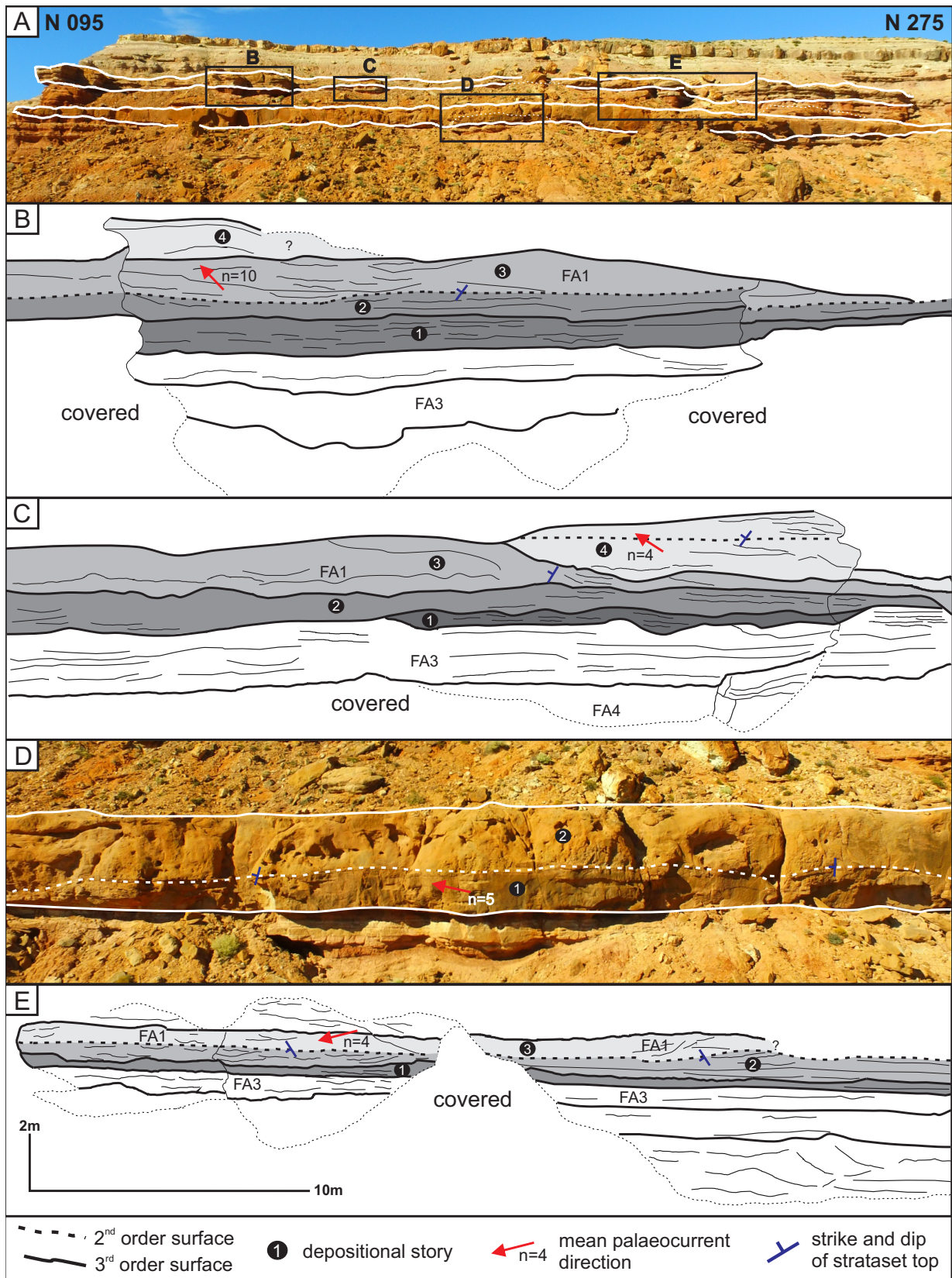


Figure 7. Architectural diagrams of low sinuosity fluvial channel deposit (FA1) of the Bardas Coloradas Member. **a)** Photomosaic of the eastern flank of the Los Chivos hill showing two fluvial bodies bounded by a third order surface, indicated with white solid lines. **b)-c)-d)- e)** Details of second and third order surfaces, paleocurrent data, and strike and dip of stratset tops. The position of these views is indicated in **a**.

Facies association	Facies	Key bounding surfaces	Geometry	Interpretation
FA1	St and Sp. Sm, Sh, and Cmm are less common	Base: erosive, concave-upward to irregular Internal: convex-upward (central bars)	Sheet or channel	Low sinuosity fluvial deposits
FA2	St and Sp. Sh, Sm, Ch, and Cmm are less frequent	Base: erosive, concave-upward to irregular Internal: lateral accretion (point bars)	Channel or ribbon	Meandering-like crevasse channel deposits
FA3	Sm and Sh. Minor participation of St, Cmm, VSm, VSh, and VSt	Base: irregular and very few erosive to non-erosive in bodies with sheet and plane-convex geometries. Internal: amalgamation	Sheet and plane-convex	Crevasse splay deposits
FA4	Mh with reduced occurrence of Sm, VSm, Mr and VMh	Base: plane and no erosive Internal: -	Sheet	Distal floodplain deposits
FA5	FA5a VSp* and VSt*	Base: non erosive and irregular Internal: -	Plane-convex	Aeolian dune deposits
	FA5b Tm and Th	Base: non erosive and irregular Internal: -	Mantle bedding	Dry-interdune deposits
	FA5c VMh and VSm	Base: non erosive and irregular Internal: -	Sheet	Wet-interdune deposits
FA6	VSm and VSt with minor amount of VSh, VSr, and VSp. Subordinated occurrence of Sm, St, Sh, and Tm	Base: erosive and irregular Internal: amalgamation	Sheet	Sheet-flood deposits
FA7	VCt and VCmm	Base: erosive and irregular Internal: -	Channel?	Volcaniclastic channel deposits

Table 2. Summary of description and interpretation of facies associations.

grained vitric tuffs with plane parallel lamination (facies Th) or massive aspect (facies Tm). Individual beds are centimeter to decimeter thick; but they can be stacked forming bodies up to ~5 m thick, which are laterally continuous for more than 100 m (Fig. 9c, d). Both Th and Tm facies commonly show accretionary lapilli (Fig. 9e), root traces (Fig. 9f), and burrows produced by invertebrates and

vertebrates, the latter including lepidosauromorphs (Pérez *et al.*, 2013b, 2015; Melchor *et al.*, 2023). The uppermost stratigraphic interval assigned to FA5b in LCh3 section can be correlated with the strata dated with U-Pb at 115.5 ± 0.14 Ma (Krause *et al.*, 2020). Finally, FA5c comprises scarce tabular bodies with non-erosive bases and a lateral continuity that exceeds 100 m, mostly constituted of laminated

Parameter (in m)	LCh1	LCh2	LCh3	
Mean thickness	3.05 m <i>n</i> = 1	3.28 m (3.20 – 3.35) <i>n</i> = 2	2.68 m (2.60 – 2.75) <i>n</i> = 2	FA1
Mean cross-set thickness (Sm) and standard deviation (StD)	-	0.2 ± 0.08 (0.18 – 0.22) <i>n</i> = 2	0.2 ± 0.09 (0.18 – 0.22) <i>n</i> = 2	
StD/Sm	-	0.40	0.43	
Mean flow depth (d) $d = 11.6 \times hm^{0.84}$ where $hm = 2.22(Sm/1.8)^{1.32}$	-	1.61 m (1.48 – 1.74) <i>n</i> = 2	1.97 m (1.76 – 2.19) <i>n</i> = 2	
Mean minimum true width (cbw min) $cbw\ min = 59.9 \times d^{1.8}$	-	142.3 m (121.5 – 163.1) <i>n</i> = 2	205.4 m (164.9 – 245.8) <i>n</i> = 2	
Mean maximum true width (cbw max) $cbw\ max = 192 \times d^{1.37}$	-	370.3 m (329 – 411.6) <i>n</i> = 2	488.7 m (415 – 562.3) <i>n</i> = 2	
Mean thickness	1.34 m <i>n</i> = 5 (1 – 1.8)	-	-	FA2
Apparent width	44.96 m <i>n</i> = 5 (21.25 – 68.63)	-	-	
Strike (azimuth)	N 275	-	-	
True width	31.56 m <i>n</i> = 5 (13.94 – 52.22)	-	-	

Table 3. Mean properties from low sinuosity fluvial channel deposits (FA1) and meandering-like crevasse channels deposits (FA2); the ranges are indicated between brackets. The bold is used to highlight the average values. The study sections at the top of the table (LCh1, LCh2 and LCh3) are referred to in Figure 3.

or massive volcaniclastic mudstones (facies VMh) together with well-sorted medium to fine-grained volcaniclastic sandstones with massive aspect (VSm) (Fig. 9g).

Interpretation. FA5 evidence aeolian sedimentation from migration of dunes separated by different types of interdune zones. In particular, FA5a represents the migration of 2D and 3D aeolian dunes by processes of grain fall and grain flow, which are recorded as facies VSp* and VSt*, respectively (Kocurek, 1996; Mountney, 2006; Pye and Tsoar, 2009). The presence of scarce root traces is compatible with weakly pedogenized deposits, indicating a relative environmental instability. FA5b represents dry interdune zones constructed from settling of suspended volcanic ash in subaerial conditions (Edgett and Lancaster, 1993; Hooper *et al.*, 2012; Melchor *et al.*, 2023).

In particular, the facies Tm suggests continuous volcanic events, whereas the facies Th indicates intermittent eruptions in which several short-lived pulses occurred (Walker, 1973; Cas and Wright, 1987; Houghton *et al.*, 2000; Petrinovic and D’Elía, 2018). The presence of accretionary lapilli records ash aggregation in the troposphere by collision between water covered particles and electrostatic attraction (Moore and Peck, 1962; Schumacher and Schmincke, 1995). Finally, the deposits were modified by organisms and pedogenesis, which are indicated by the presence of burrows and root traces. On the other hand, FA5c shows local development of a wet interdune environment suggested by alternate sediment settling in standing waters (facies VMh) and stream-currents that formed sediment-laden flows (facies VSm).

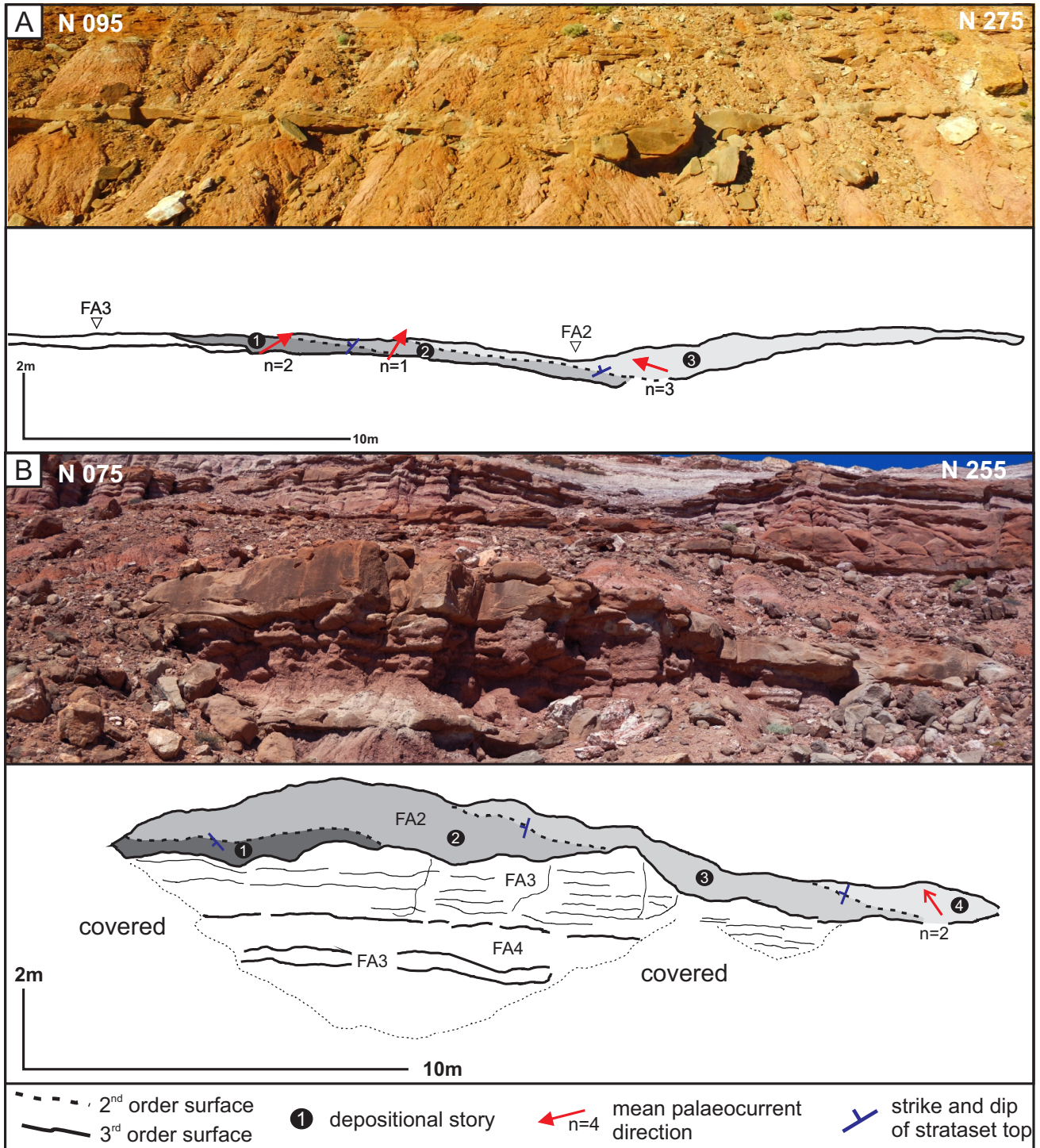


Figure 8. Architectural diagrams of meandering-like crevasse channel deposits (FA2). **a)-b)** Arrangement of second and third order surfaces, paleocurrent data, and strike and dip of stratset tops.

Sheet-flood deposits (FA6)

FA6 consists of sheet-like bodies mostly composed of medium to fine-grained volcanoclastic sandstones which laterally change into volcanoclastic mudstones

(Fig. 10a). The volcanoclastic sandstones have irregular and slightly erosive bases and are mainly massive (facies VSm) or exhibit trough cross-bedding (facies VSt). In minor proportion, the volcanoclastic sandstones show plane parallel lamination (facies

VSh) (Fig. 10b), ripple cross-lamination (facies VSr), and tabular planar cross-bedding (facies VSp). In addition, there is subordinate participation of medium to fine-grained sandstones, which are commonly massive (facies Sm), or less frequently exhibiting trough cross-bedding (facies St) and plane parallel lamination (facies Sh). The alternation of massive and laminated or cross-bedded strata is common. The volcaniclastic mudstones show no erosive bases, plane parallel lamination, and occasional desiccation cracks, or show massive aspect due to bioturbation (facies VMh). There is very rare occurrence of centimeter thick layers of massive tuffs (facies Tm) with very limited lateral continuity. Individual beds have decimeter to meter thick but are amalgamated or vertically stacked conforming bodies up to ~22 m thick and laterally continuous for up to several hundred meters. The occurrence of burrowed and rooted strata is common.

Interpretation. FA6 records sheet-floods with abundant volcaniclastic-rich sediment composition (Cas and Wright, 1987; Martina *et al.*, 2006; Fisher *et al.*, 2007; Hampton and Horton, 2007; Nichols and Fisher, 2007; Umazano *et al.*, 2008, 2012, 2017). The massive sandstone facies (VSm and Sm) indicate deposition from sediment-laden flows in which bedforms are not formed or preserved. The remaining sandstone facies are compatible with plane bed conditions (facies VSh and Sh) and migration of different types of bedforms including ripples (VSr) and dunes with straight (VSp) or sinuous crests (VSt). The common upward change from massive beds to laminated or cross-bedded strata is interpreted as dilution phenomena. Therefore, the massive sandstone beds could represent more proximal positions of the sheet-floods, whereas the laminated or cross-bedded sandstone strata would indicate more distal zones (Umazano *et al.*, 2017). On the other hand, the mudstone parts (facies VMh) indicate a very shallow lake to ponded environment in which settling of fine-grained volcaniclastic-rich suspended sediments occurred (Talbot and Allen, 1996; Nakayama and Yoshikawa, 1997). The facies Tm represents local traces of subaerial settling of volcanic ash. Locally, FA6 deposits were modified by pedogenesis or biologically altered by burrowing animals.

Volcaniclastic channel deposits (FA7)

FA7 is represented by a single volcaniclastic-rich conglomerate-dominated body with subtle finning-upward trend. The base is irregular and erosive, and the top is horizontal (Fig. 10c, d). The geometry and internal bounding surfaces could not be observed. It is mainly composed of an alternation of volcaniclastic breccias with the following main features: i) moderately well sorting and trough cross-bedding (facies VCt); and ii) very poor sorting and massive, matrix-supported aspect (facies VCmm). In both facies, the clasts are tuff fragments, and the matrix is fine-grained ash. The uppermost part of the body is represented by a decimeter thick, coarse to medium-grained sandstone bed with trough cross-bedding (facies St). Mean paleocurrent data from facies VCt indicates a paleoflow towards NW.

Interpretation. According to the constituent facies, erosive base, and finning-upward trend, FA7 is considered a fluvial channel deposit (Miall, 1996; Bridge, 1993, 2003, 2006; Gibling, 2006; Paredes, 2022). The sedimentation occurred in the context of perennial flows including deposition from volcaniclastic debris-flows (facies VCmm) and reworking of resulting deposits by dilute currents, which originated the facies VCt and St, respectively. The channel pattern is uncertain, but the constituent facies suggest a low sinuosity plan-view.

ARCHITECTURE OF FACIES ASSOCIATIONS

According to the spatial-temporal distribution of facies associations, the studied successions were divided into three informal stratigraphic intervals named A, B and C in chronological order of deposition. Their boundaries are the Bardas Coloradas – Puesto La Paloma boundary and a continuous marker bed which represents pedogenized ash-fall deposits included within FA5b (Fig. 11a, b). Figure 12 shows the ratio of each facies association in the stratigraphic intervals.

The stratigraphic interval A (up to 35 m thick) corresponds to the Bardas Coloradas Member (Fig. 11a, b). It includes an alternation of both low sinuosity (FA1) and meandering-like (FA2) fluvial channel deposits, with distal floodplain (FA4) or crevasse splay (FA3)

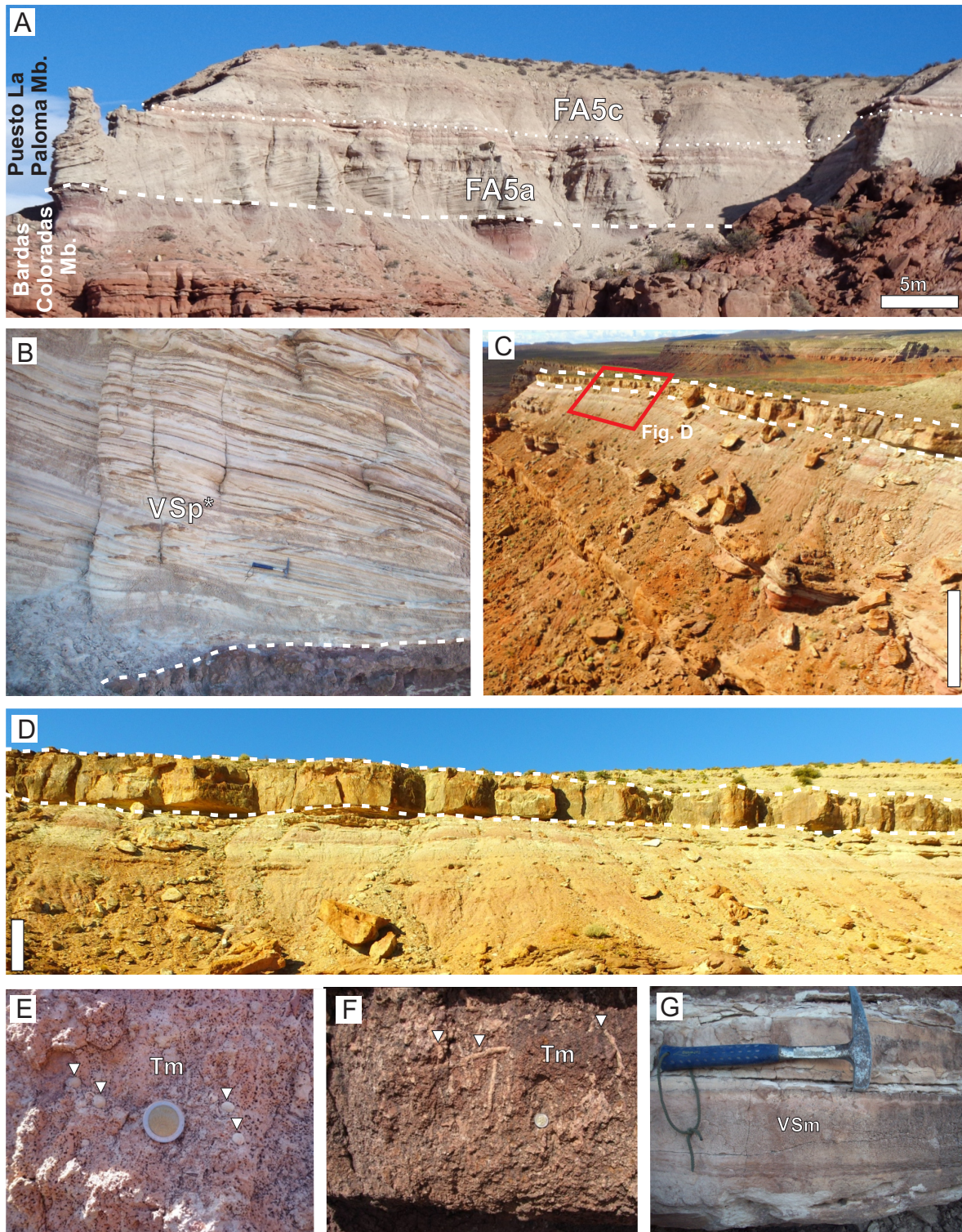


Figure 9. Examples of aeolian deposits (FA5) recognized in the lower Puesto La Paloma Member. **a)** Panoramic view of aeolian dune deposits (FA5a) underlying wet interdune deposits (FA5c) close the boundary between Bardas Coloradas and Puesto La Paloma members. **b)** Detail of cross-bedded volcanoclastic sandstones (facies VSp*) of aeolian origin (FA5a). The base is indicated using a dotted line. **c-d)** Panoramic view and detail of a body with mantle bedding composed of fine-grained tuff (facies Tm), included in dry interdune deposits (FA5b). Base and top are marked using dotted lines. Scale bars are 10 and 2 m long, respectively. **e)** Detail of a massive tuff (facies Tm) bearing accretionary lapilli (white triangles) in FA5b deposits. **f)** Detail of a massive tuff (facies Tm) with root traces (white triangles) in FA5b deposits. **g)** Detail of massive volcanoclastic sandstone (facies VSm) included in wet interdune deposits (FA5c). In b) and g) the hammer is 0.33 m long, and in e) and f) the coin is 2.25 cm in diameter.

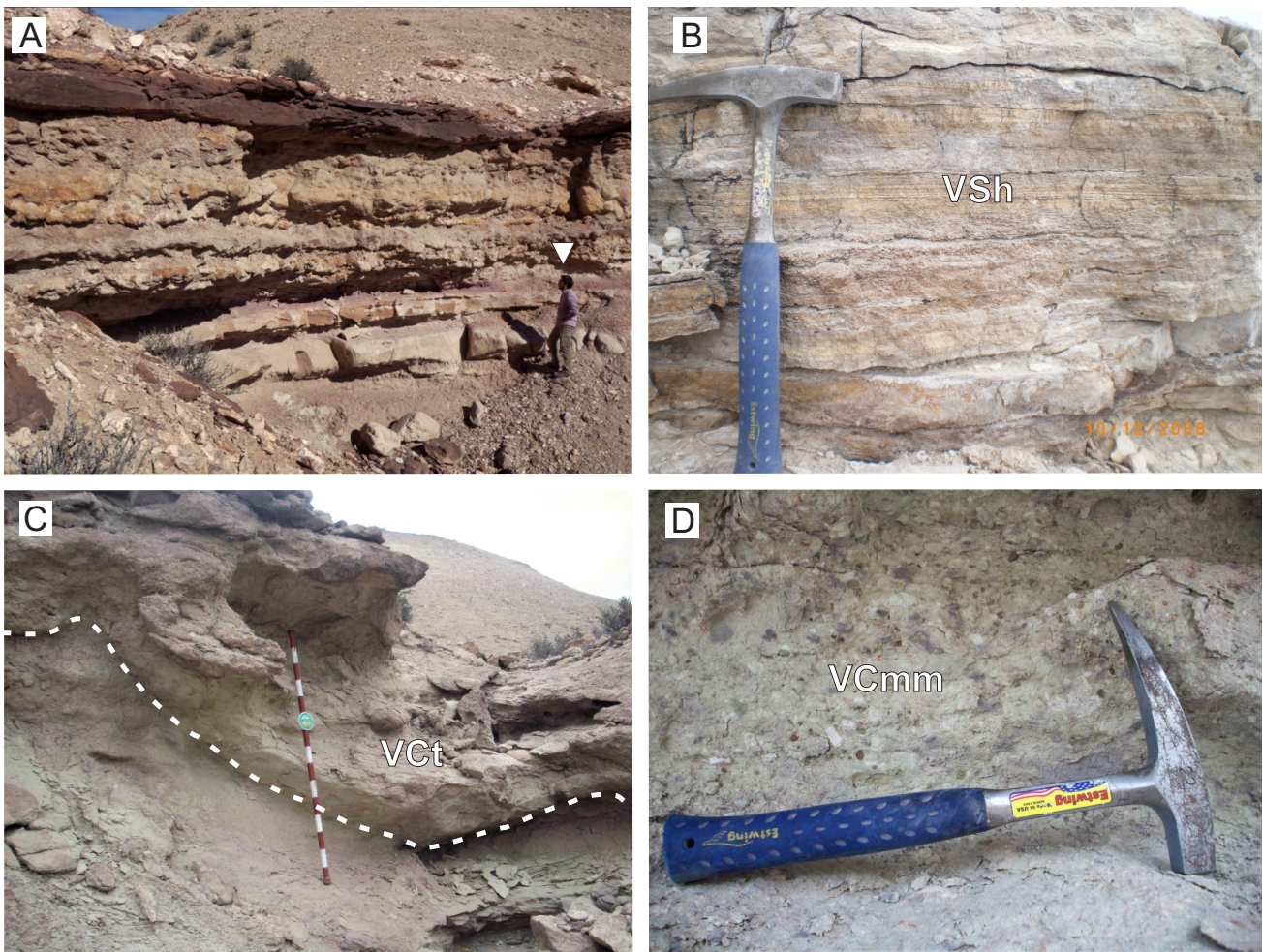


Figure 10. Examples of reworked volcaniclastic facies associations recognized in the middle-upper Puesto La Paloma Member. **a)** Alternation of volcaniclastic sandstones with horizontal lamination (facies VSh) and massive aspect (facies VSm) (FA6). Person for scale (white triangle). **b)** Detail of laminated volcaniclastic sandstones (facies VSh) (FA6). **c)** Trough cross-bedded volcaniclastic conglomerates (facies VCt) overlying an irregular and erosive surface indicated with a dashed line (FA7). Jacob staff is 1.50 m long. **d)** Massive and matrix supported volcaniclastic conglomerate (facies VCmm) assigned to FA7. Hammer in b) and d) is 0.33 m long.

deposits (Fig. 12). In the lower part of this stratigraphic interval, the fluvial channel bodies are commonly encased in distal floodplain deposits and represents crevasse-channels. On the other hand, the upper part of the stratigraphic interval comprises low sinuosity fluvial channel deposits. These are isolated or amalgamated and enclosed in a large number of crevasse splay deposits.

The stratigraphic interval B (11-16 m thick) transitionally overlies the interval A and characterizes the lower part of the Puesto La Paloma Member (Fig. 11a, b). Its lower boundary is located where the succession is completely volcaniclastic and its upper one corresponds to the tuff marker bed. Stratigraphic interval B is composed of aeolian

deposits (FA5), including the local occurrence of dunes (FA5a) (Fig. 12), which are vertically and laterally associated with interdune zones, both wet (FA5c) and dry (FA5b), with dominant and reduced participation respectively.

The stratigraphic interval C (6-18 m thick) includes the upper part of the Puesto La Paloma Member (Figs. 11a, b). The lower boundary is a smoothly irregular surface that in places is erosive on the underlying tuffaceous marker bed, whereas the upper boundary coincides with the Puesto La Paloma / Cerro Castaño contact. It is basically constituted by sheet-flood deposits (FA6) with a unique, isolated volcaniclastic channel deposit (FA7) (Fig. 12).

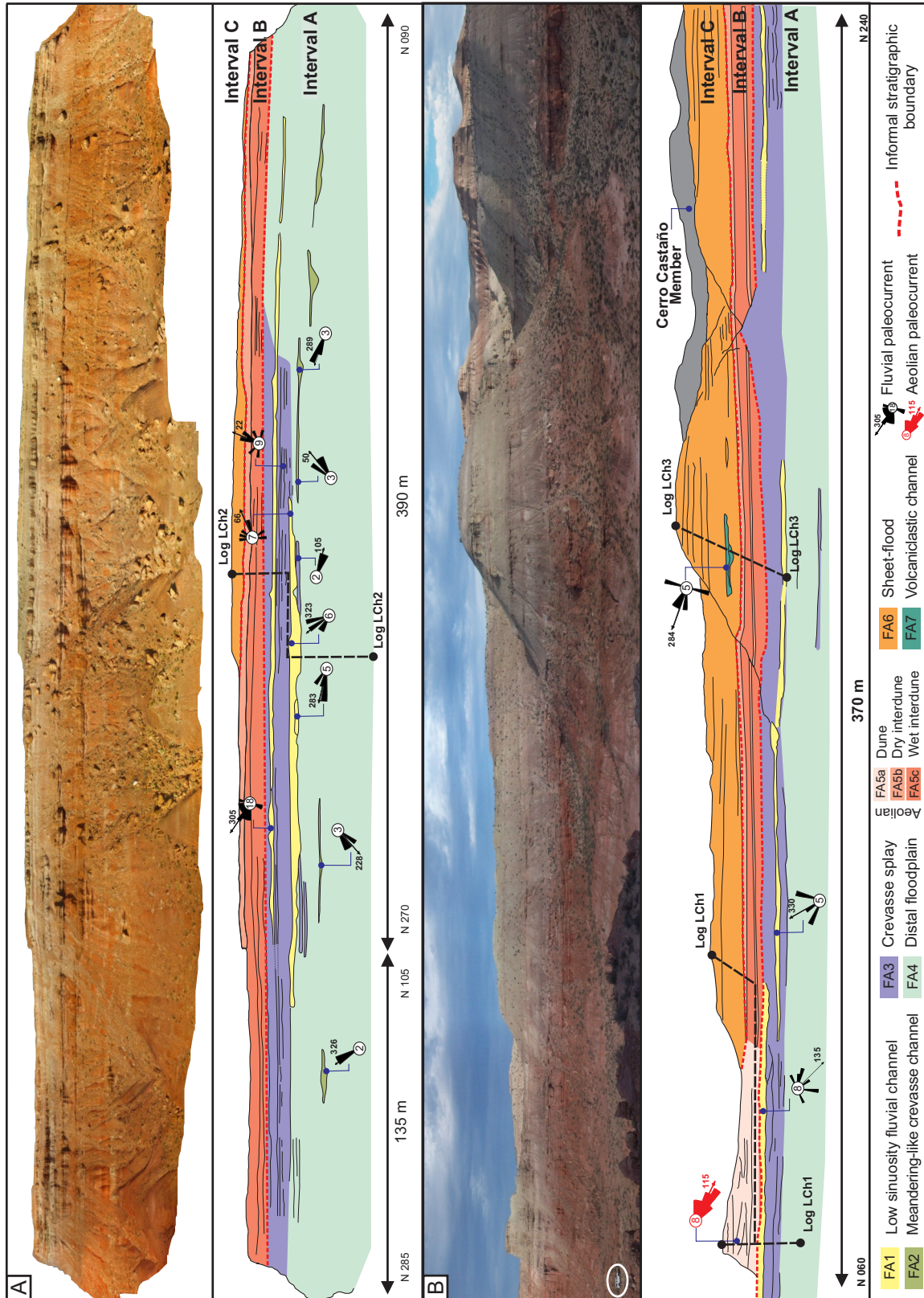


Figure 11. Facies architecture of the Bardas Coloradas and Puesto La Paloma members at Los Chivos hill. **a)** Photomosaic of the three informal stratigraphic intervals at the eastern flank of the Los Chivos hill showing the trace of log LCh2 and the different facies associations with their main bounding surfaces, paleocurrent data, and boundary between informal stratigraphic intervals. **b)** Photomosaic of vertical and lateral relationships between the facies associations recognized including trace log of sites LCh1 and LCh3.

DEPOSITIONAL MODEL

The schematic diagrams of figure 13 summarize the evolution of inferred depositional environments. The stratigraphic interval A was deposited in a fluvial environment with scarce influx of volcaniclastic sediments (Fig. 13a). In particular, the main fluvial channels were of low sinuosity, perennial, characterized by dilute flows with sand-dominated bed loads (FA1), and with a general drainage towards NW. The adjacent floodplains were vegetated and dominated by crevasse splays (FA3) and settling of suspended sediments in standing water (FA4). The vertical and lateral facies arrangement suggests that overbank flows were diluted with increasing distance from the main channels, until reaching distal parts of the floodplain where shallow lakes or ponded zones were located. In addition, the transfer of water and sediment from the main channels to the floodplain also occurred through meandering-like crevasse-channels (FA2), which were frequently drained by dilute flows with large fluctuations in water discharge. Scarce debris flow deposits, both in fluvial channel and floodplain zones, represent the very occasional occurrence of more concentrated flows. The episodic nature of the floodplain sedimentation is marked by the presence of massive paleosol levels without differentiation of horizons.

The stratigraphic interval B records sedimentation in an aeolian system with recurrent volcaniclastic influx (Fig. 13b). The sediment was delivered by ash-fall events and the resulting deposits covered the topography uniformly and were either preserved and pedogenized in dry interdune zones (FA5b) or reworked by wind and water. The aeolian reworking formed 2D dunes with minor scale superimposed 3D dunes (FA5a), which migrated south-eastwards by grain fall and grain flow processes. The discontinuous sedimentation of the aeolian dunes is indicated by the presence of reactivation surfaces and paleosols. There were few places in the interdune zone with small topographic depressions where deposition of suspended sediments occurred in standing water; probably very rare sediment-laden flows reached them (FA5c).

The stratigraphic interval C records mainly volcaniclastic sheet-floods deposits generated

by the fluvial reworking of primary volcaniclastic deposits, such as the tuffaceous marker bed (Fig. 13c). The sheet-floods constituted a continuum characterized by sediment-laden flows in proximal sectors which, progressively evolved to typical stream currents that supplied very shallow lakes or ponded zones (FA6). These sheet-floods had probably an additional and local source by a volcaniclastic channel (FA7), which is considered a feeder-like channel that drained from the southern sector of the depocenter. As in the previous stratigraphic intervals A and B, the presence of apedal paleosol levels without horizonation suggests the episodic nature of sedimentation.

CONTROL FACTORS ON FLUVIAL ARCHITECTURE

In this section, we analyse the potential influence of tectonic activity, climate change, and volcaniclastic sediment supply on fluvial sedimentation. The influence of the eustatic sea-level changes was discarded since the analysed succession was deposited without oceanic connection (Smith *et al.*, 1981; Cortiñas, 1996; Figari *et al.*, 2015; Gianni *et al.*, 2015; Allard *et al.*, 2022; Figari and Hechem, 2022). On the other hand, the basement morphology control was assumed negligible because the analysed sections are not overlying a paleorelief, which in fact, is a common situation in several sectors of the basin overlying Jurassic volcanic rocks (Figari *et al.*, 2015; Umazano *et al.*, 2017; Villegas *et al.*, 2019; Krause *et al.*, 2020; Allard *et al.*, 2022; Villegas, 2022).

Tectonic activity

The analysed successions are located in the southern sector of the Gorro Frigio depocenter, particularly in a depositional zone limited by two inverted faults with NE-SW orientation (Fig. 3) and planes that dip towards the NNW (Figari *et al.*, 2015; Allard *et al.*, 2022). Considering this structural scenario, the mean paleocurrent estimated from the main fluvial channel deposits of stratigraphic interval A, as well as most of the mean paleocurrents of individual bodies, suggest a transversal-like fluvial system (Gawthorpe and Leeder, 2000; Bridge, 2003). The dissimilar mean paleocurrent of the uppermost fluvial

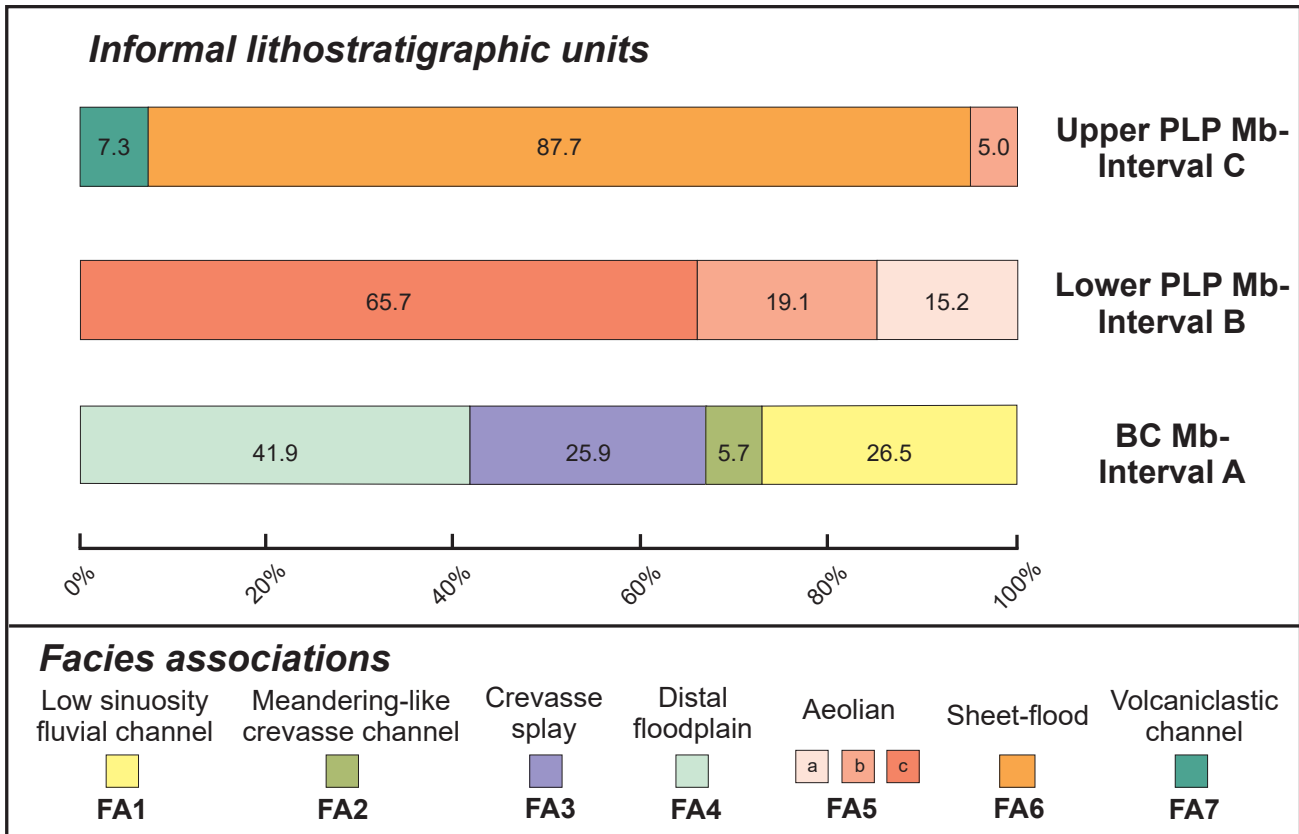


Figure 12. Percentage of participation of each facies association per informal stratigraphic interval. The percentages were calculated from the measured total thickness.

channel body in LCh3 section (Fig. 5) could represent a low-hierarchy fluvial course or, alternatively, a reversed drainage due to uplifting footwalls (Gawthorpe and Leeder, 2000). The lack of correlation with other indicators of syn-tectonic sedimentation, including fluvial paleochannels that vary in thickness in relation to syn-sedimentary deformational structures or variations in sediment composition (Bridge 2003, 2006; Paredes, 2022), make the syn-tectonic explanation of this feature unlikely.

The stratigraphic intervals B and C, which represent aeolian and unconfined fluvial conditions, respectively, also show no evidence of tectonic activity penecontemporaneous with the sedimentation, such as progressive discordances and growth strata. In a regional context characterized by thermal subsidence with subordinate and local extensional control, this period of tectonic quiescence is also evidenced in other areas of the Gorro Frigio depocenter, even near the inverted master fault (Figari *et al.*, 2015; Allard *et al.*, 2022). The mean paleocurrent

for the volcaniclastic channel deposit included in stratigraphic interval C is consistent with the general drainage established for the underlying stratigraphic interval A.

Climate change

There is scarce information from the analyzed successions pointing to precise paleoclimatic inferences. Nevertheless, by combining some proxies with published data, the climatic background can be estimated. Deposition of stratigraphic interval A occurred in semiarid-arid conditions. This inference is supported by: i) the quantitative paleohydrologic estimations from thickness of cross-bedded sandstones of fluvial channel deposits, which suggest paleoprecipitations of ~350 mm/year (Allard *et al.*, 2022); ii) the presence of calcium carbonate and gypsum concentrations in paleosols (De Sosa Tomas *et al.*, 2022); and iii) the record of carbonatic lacustrine deposits in floodplain successions which bear particular charophyte assemblages (De Sosa Tomas *et al.*, 2022). A seasonal climate in upstream

positions is envisaged from the record of perennial fluvial channels with evidence of important variations in water discharge (Brea *et al.*, 2016; Allard *et al.*, 2022). The coexistence of calcic and hydromorphic features in associated floodplain paleosols also indicates alternation of drier and wetter seasons (De Sosa Tomas *et al.*, 2022). Moreover, the sedimentologic data presented in this contribution does not include facies with contrasting climatic significance in floodplain deposits (*e.g.*, coal, evaporites and aeolianites) suggesting stable climatic conditions during deposition of stratigraphic interval A (cf. Glennie, 1987; Langford and Chan, 1989; Smoot and Lowenstein, 1991; Parrish, 1998).

The stratigraphic intervals B and C were also deposited in seasonal semiarid-arid climatic conditions. This interpretation is mainly based on the common record of amalgamated and pedogenized unconfined fluvial deposits, which represent the typical sedimentary facies of the Puesto La Paloma Member on a basin scale, in many places with scarce intercalations of carbonatic lacustrine facies (Brea *et al.*, 2016; Umazano *et al.*, 2017; Krause *et al.*, 2020). This is consistent with the mean annual precipitation values ranging from ~200 to ~700 mm/year obtained using geochemical data from paleosols along complete sections of the unit, which are compatible with the low degree of chemical weathering of tuffaceous deposits (Krause *et al.*, 2014). As in the underlying stratigraphic interval, the seasonality is inferred from the overlapping of hydromorphic and calcification features in paleosols (Krause *et al.*, 2014). Although interval B is characterized by a volcaniclastic aeolian system, such feature is restricted to the western sector of the basin defined upon sedimentary records of nearby localities separated up to ~10 km (see Umazano *et al.*, 2017). The restricted distribution of these deposits, combined with the mean paleocurrent direction, suggests a local paleotopographic condition linked to sedimentary corridors (Allard *et al.*, 2022). Thus, the recognition of climatic temporal trends is uncertain and further studies would be needed.

Volcaniclastic sediment supply

The participation of volcaniclastic detritus is represented as scarce thin intercalations in the stratigraphic interval A, while it represents most of the stratigraphic intervals B and C, suggesting

a temporal increase in the volcaniclastic sediment supply. In general, this major participation of volcaniclastic detritus during deposition of Puesto La Paloma Member has been addressed in the western sector of the basin (Codignotto *et al.*, 1978; Figari *et al.*, 2015; Krause *et al.*, 2020; Figari and Hechem, 2022; Allard *et al.*, 2022). In this regional context and considering the absence of evidence for unequivocal important climatic changes and tectonic activity during deposition of the analysed successions, the modification of the sedimentary paleoenvironments and depositional architecture could be linked with the temporal variability in volcaniclastic sediment supply. In particular, the modification from fluvial (interval A) to aeolian (interval B) conditions, could be related with a sudden increase in the input of volcaniclastic sediments. This elevated influx produced an overfed sedimentary system with the consequent high availability of surface deposits that were susceptible of being reworked by aeolian dunes, a well-documented situation in fluvial environments highly impacted by volcaniclastic influx in both humid and arid climatic conditions (Edgett and Lancaster, 1993; Umazano *et al.*, 2014, 2021). Thus, the stratigraphic interval B recorded in Los Chivos hill represents local conditions of a very complex and slightly extensive aeolian system.

On the other hand, the overlying stratigraphic interval C, which records unconfined fluvial conditions with common development of sediment laden flows, is interpreted as sedimentation affected by a high volcaniclastic influx (Smith and Lowe, 1991; Umazano *et al.*, 2017; Villegas, 2022). In this case, the volcaniclastic input favoured the sheet-flood development suggesting a high transport rate within the sedimentary system or conditions of extreme aggradation (Manville *et al.*, 2009; Pierson and Major, 2014). Compared to interval B, the development of sheet-floods instead of aeolian dunes suggests a minor availability of unconsolidated surface sediments, which in a context of sedimentary corridors would be related to less erosion from the slopes.

CONCLUSIONS

The sedimentological study of the Cretaceous Bardas Coloradas and Puesto La Paloma members (Somuncurá-Cañadón Asfalto Basin, Patagonia,

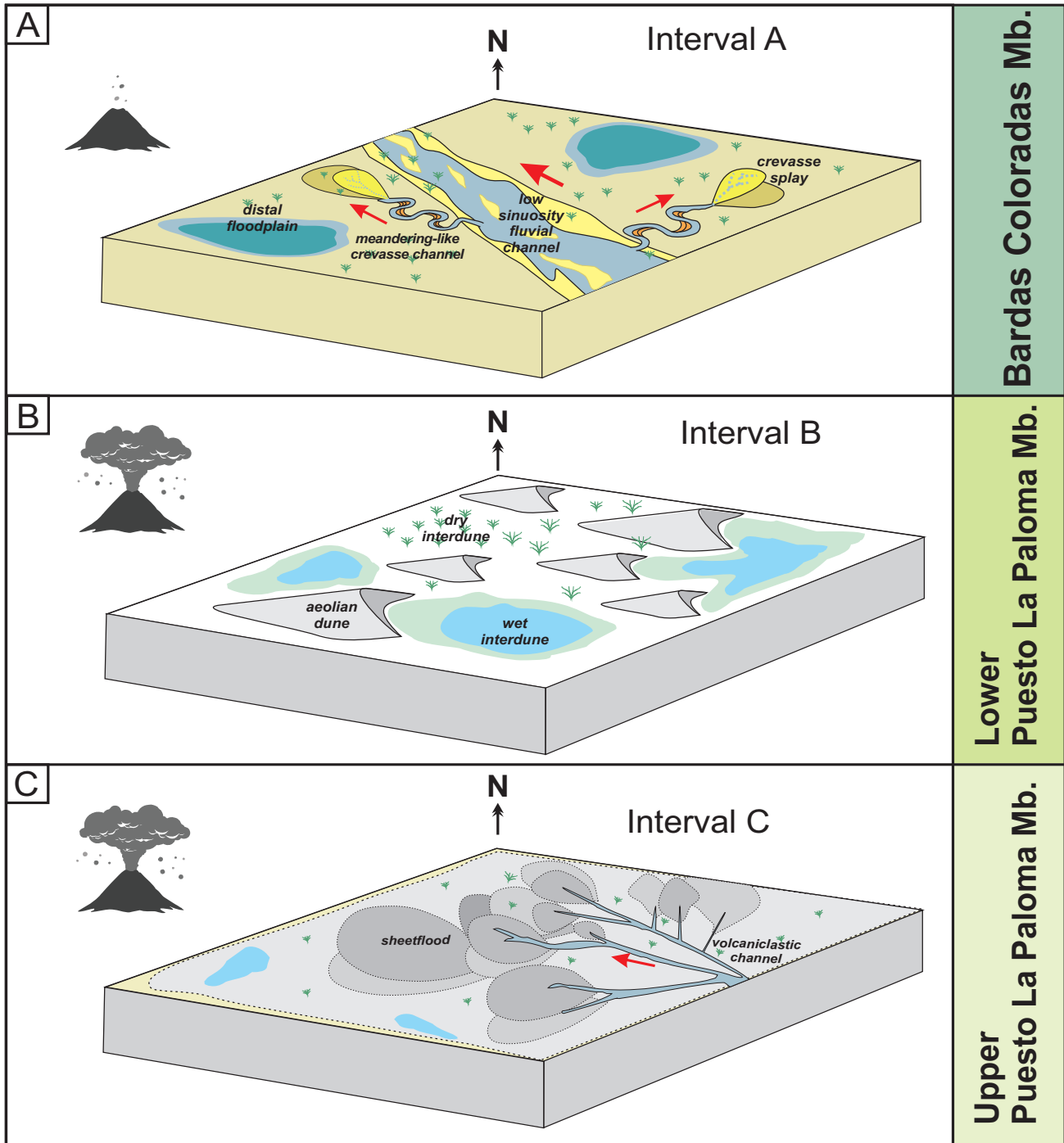


Figure 13. Paleoenvironmental reconstruction of the Bardas Coloradas and Puesto La Paloma members in the study area. **a)** Stratigraphic interval A (Bardas Coloradas Member). **b)** Stratigraphic interval B (lower Puesto La Paloma Member). **c)** Stratigraphic interval C (upper Puesto La Paloma Member). The red arrows indicate the mean paleoflow from fluvial channel deposits.

Argentina) employing both facies and body-scale architectural analysis, together with their spatial-temporal relationships (alluvial stratigraphy), allowed determining three informal intervals according with the occurrence of different facies associations. Based on this, we reach to the following main conclusions.

The lower stratigraphic interval A (Bardas Coloradas Member) represents a fluvial system with rare volcaniclastic sediments. It includes low sinuosity main fluvial channels, which mostly transported a sandy bedload towards NW, and vegetated floodplain areas characterized by the

presence of meandering-like crevasse channels, crevasse splays and shallow lakes or ponded zones.

The stratigraphic interval B (lower Puesto La Paloma Member) records a volcaniclastic aeolian system composed of 2D aeolian dunes that migrated towards SE, which were spatially related to wet- and dry-interdune zones where the sedimentation mostly occurred from subaqueous and subaerial settling of suspended volcaniclastic sediments, respectively.

The stratigraphic interval C (upper Puesto La Paloma Member) records volcaniclastic fluvial sedimentation characterized by unconfined flows, which were sediment-laden or diluted, showing lateral relationships with ponded areas where the sedimentation mainly occurred by settling of fine-grained volcaniclastic suspended sediments. Locally, there was a volcaniclastic channel that transported volcaniclastic gravels towards NW.

The evaluation of all possible allocyclic factors suggests that changes in the amount of the volcaniclastic sediment supply governed the changes in the sedimentary environments and their architecture. The Bardas Coloradas Member represents a channelized fluvial system with scarce volcaniclastic influx that did not cause major modifications in the sedimentary system (pre-eruptive). The Puesto La Paloma Member records aeolian and fluvial conditions where the sedimentation was driven by the volcaniclastic sedimentary influx (syn- to early post-eruptive). This occurred in a context of tectonic quiescence, probably uniform semi-arid climate, and lack of influence of eustatic sea-level or basement morphology.

Acknowledgements

This study was funded by the Project 16G of the Facultad de Ciencias Exactas y Naturales of Universidad Nacional de La Pampa conducted by A.M. Umazano, as well as by the Project PICT 2019-00114 and PIP 146 conducted by Ricardo Néstor Melchor. Graciela Visconti, Mariano Pérez, Emilio Bedatou, and Pablo Puerta helped during the field work. The paleoclimatic inferences of a previous version were improved after comments from Javier Marcelo Krause. The logistic support of the Comisión Nacional de Energía Atómica (CNEA) was very valuable. Comments and suggestions from Manuel Lopez and an anonymous reviewer greatly

improved the final quality of the manuscript. The editorial assistance of José I. Cuitiño is sincerely appreciated.

REFERENCES

- Allard, J.O., Paredes, J.M., and Giacosa, R.E. (2009). *Fluvial dynamics, alluvial architecture and palaeohydrology of axial and transverse drainage systems in an extensional setting: Los Adobes Formation (Aptian), Cañadón Asfalto Basin, Argentina*. IX International Conference on Fluvial Sedimentation: 12–13, Tucumán.
- Allard, J.O., Paredes, J.M., and Giacosa, R.E. (2010a). *Recognition of tectonic, climatic and geomorphic signals in a fluvial succession developed in an extensional setting: Los Adobes Formation (Aptian) in the Cañadón Asfalto Basin, Argentina*. XVIII International Sedimentological Congress: 102, Mendoza.
- Allard, J.O., Paredes, J.M., and Giacosa, R.E. (2010b). *Spatial variability in the external geometry (W/t ratio) of fluvial channels and its implications for basin analysis and reservoir characterization: Los Adobes Formation (Aptian) of the Cañadón Asfalto Basin, Central Patagonia*. XVIII International Sedimentological Congress: 103, Mendoza.
- Allard, J.O., Giacosa, R.E., and Paredes, J.M. (2011). *Relaciones estratigráficas entre la Formación Los Adobes (Cretácico Inferior) y su sustrato Jurásico: implicancias en la evolución tectónica de la Cuenca de Cañadón Asfalto, Chubut, Argentina*. XVIII Congreso Geológico Argentino: 988-989, Neuquén.
- Allard, J.O., Paredes, J.M., Foix, N., and Giacosa, R.E. (2012). *Un test sedimentológico para establecer el límite entre las cuencas de Cañadón Asfalto y del Golfo San Jorge durante la depositación del Grupo Chubut (Cretácico): implicancias paleogeográficas de datos de paleoflujos*. XIII Reunión Argentina de Sedimentología: 241-242, Salta.
- Allard, J.O., Paredes, J.M., Foix, N., and Giacosa, R.E. (2014). *Depósitos aluviales de la Formación Cerro Barcino en el borde nororiental de la Cuenca de Cañadón Asfalto: interpretación paleoambiental, evolución temporal y evidencias de actividad tectónica sinsedimentaria*. XIX Congreso Geológico Argentino: 18-19, Córdoba.
- Allard, J.O., Paredes, J.M., Giacosa, R.E., and Foix, N. (2015). *Conexión cretácica entre las cuencas del Golfo San Jorge y Cañadón Asfalto (Patagonia): implicancias tectonoestratigráficas y su potencial en la exploración de hidrocarburos*. *Revista de la Asociación Geológica Argentina*, 72: 21-37.
- Allard, J.O., Paredes, J.M., Foix, N., Giacosa, R.E., Buetti, S., and Sánchez, F. (2022). *Estratigrafía de la cuenca Cañadón Asfalto*. In: Giacosa, R.E. (Ed.): *Geología y Recursos Naturales de la Provincia del Chubut*. Relatorio del XXI Congreso Geológico Argentino: 187-265.
- Allen, J.R.L. (1983). *Studies in fluvial sedimentation: Bars, bar-complexes and sandstone sheets (low-sinuosity braided streams) in the Brownstones (L. Devonian), Welsh Borders*. *Sedimentary Geology*, 33(4): 237-293.
- Best, J.L., and Bristow, C.S. (1993). *Braided Rivers*. Geological Society Special Publication 75, London, 419 pp.
- Brea, M., Bellosi, E.S., Umazano, A.M., and Krause, J.M. (2016). *Aptian-Albian Cupressaceae (sensu stricto) woods from Cañadón Asfalto Basin, Patagonia Argentina*. *Cretaceous Research*, 58: 17-28.

- Bridge, J.S. (1993). Description and interpretation of fluvial deposits: a critical perspective. *Sedimentology*, 40: 801-810.
- Bridge, J.S. (2003). *Rivers and Floodplains: Forms, Processes and Sedimentary Record*. Blackwell Scientific Publications, Oxford, 491 pp.
- Bridge, J.S. (2006). Fluvial facies models: recent developments. In: Posamentier, H.W., Walker, R.G. (Eds.), *Facies Models Revisited*. Society of Economic Paleontologists and Mineralogists, Special Publication 84: 85-170.
- Bridge, J.S. and Mackey, S.D. (1993). A theoretical study of fluvial sandstone body dimensions. In: Flint, S. and Bryant, I.D. (Eds): *The Geological Modeling of Hydrocarbon Reservoirs*. International Association of Sedimentologists Special Publication, 15: 213-236.
- Bridge, J.S., and Tye, R.S. (2000). Interpreting the dimensions of ancient fluvial channel bars, channels, and channel belts from wireline-logs and cores. *American Association of Petroleum Geologists Bulletin*, 84: 1205-1228.
- Bridge, J.S. and Lunt, I.A. (2006). Depositional models of braided rivers. In: Sambrook Smith, G.H., Best, J.L., Bristow, C.S., Petts, G. (Eds.), *Braided Rivers II*: 11-50.
- Bridge, J.S., and Demicco, R. (2008). *Earth Surface Processes, Landforms and Sediment Deposits*. Cambridge University Press, 815 pp.
- Bridge, J.S., Jalfin, G.A., and Georgieff, S.M. (2000). Geometry, lithofacies, and spatial distribution of Cretaceous fluvial sandstone bodies, San Jorge basin, Argentina: outcrop analog for the hydrocarbon-bearing Chubut Group. *Journal of Sedimentary Research*, 70: 341-359.
- Bristow, C.S., Skelly, R.L., and Ethridge, F.G. (1999). Crevasse splays from the rapidly aggrading, sand-bed, braided Niobrara River, Nebraska: effect of base-level rise. *Sedimentology*, 46: 1029-1047.
- Burns, C.E., Mountney, N.P., Hodgson, D.M., Colombera, L. (2017). Anatomy and dimensions of fluvial crevasse-splay deposits: Examples from the Cretaceous Castlegate Sandstone and Neslen Formation, Utah, U.S.A. *Sedimentary Geology*, 351: 21-35.
- Butler, K.L., Horton, B.K., Echaurren, A., Folguera, A., and Fuentes, F. (2020). Cretaceous-Cenozoic growth of the Patagonian broken foreland basin, Argentina: Chronostratigraphic framework and provenance variations during transitions in Andean subduction dynamics. *Journal of South American Earth Sciences*, 97: doi.org/10.1016/j.jsames.2019.102242.
- Carmona, R.P., Umazano, A.M., and Krause, J.M. (2016). Estudio estratigráfico y sedimentológico de las sedimentitas portadoras de los titanosaurios gigantes del Albiano Tardío de Patagonia central, Argentina. *Latin American Journal of Sedimentology and Basin Analysis*, 23(2): 127-132.
- Cas, R.A.F. and Wright, J.V. (1987). *Volcanic Successions: Modern and Ancient*. Allen and Unwin, London, 528 pp.
- Catuneanu O., Abreu, V., Bhattacharya, J.P., Blum, M.D., Dalrymple, R.W., Eriksson, P.G., Fielding, C., Fisher, W.L., Galloway, W.E., Gibling, M.R., Giles, K.A., Holbrook, J.M., Jordan, R., Kendall, C.G.St.C., Macurda, B., Martinsen, O.J., Miall, A.D., Neal, J.E., Nummedal, D., Pomar, L., Posamentier, H.W., Pratt, B.R., Sarg, J.F., Shanley, K.W., Steel, R.J., Strasser, A., Tucker, M.E., and Winker, C. (2009). Towards the standardization of sequence stratigraphy. *Earth-Science Reviews*, 92: 1-33.
- Cladera, G., Limarino, C.O., Alonso, M.S., and Rauhut, O. (2004). Controles estratigráficos en la preservación de restos de vertebrados en la Formación Cerro Barcino (Cenomaniano), provincia de Chubut. *Revista de la Asociación Argentina de Sedimentología*, 11: 39-55.
- Codignotto, J., Nullo, F., Panza, J., and Proserpio, C. (1978). *Estratigrafía del Grupo Chubut, entre Paso de Indios y Las Plumas, Chubut*. VII Congreso Geológico Argentino: 471-480, Neuquén.
- Cortiñas, J.S. (1996). *La cuenca de Somuncurá-Cañadón Asfalto: sus límites, ciclos evolutivos del relleno sedimentario y posibilidades exploratorias*. XIII Congreso Geológico Argentino and III Congreso de Exploración de Hidrocarburos: 147-163, Buenos Aires.
- Critelli, S., Criniti, S., Ingersoll, R.V., and Cavazza, W. (2023). Temporal and spatial significance of volcanic particles in sand (stone): implications for provenance and palaeotectonic reconstructions. In: Di Capua, A., De Rosa, R., Kereszturi, G., Le Pera, E., Rosi, M. and Watt, S. F. L. (Eds.), *Volcanic Processes in the Sedimentary Record: When Volcanoes Meet the Environment*. Geological Society, London, Special Publications, 520: 311 - 325.
- Cuitiño, J.I., and Scasso, R.A. (2013). Reworked pyroclastic beds in the early Miocene of Patagonia: Reaction in response to high sediment supply during explosive volcanic events. *Sedimentary Geology* 289: 194-209.
- Cúneo, R., Ramezani, J., Scasso, R.A., Pol, D., Escapa, I., Zavattieri, A.M., and Bowring, S. (2013). High-precision U-Pb geochronology and a new chronostratigraphy for the Cañadón Asfalto Basin, Chubut, central Patagonia: implications for terrestrial fauna. *Gondwana Research*, 24: 1267-1275.
- de la Fuente, M.S., Umazano, A.M., Sterli, J., and Carballido, J.L. (2011). New chelid turtles of the lower section of the Cerro Barcino Formation (Aptian-Albian?), Patagonia, Argentina. *Cretaceous Research*, 32: 527-537.
- De Sosa Tomas, A., Vallati, P., Martín-Closas C. (2017). Biostratigraphy and biogeography of charophytes from the Cerro Barcino Formation (upper Aptian-lower Albian), Cañadón Asfalto Basin, central Patagonia, Argentina. *Cretaceous Research*, 79: 1-11.
- De Sosa Tomas, A., Martín-Closas, C., Vallati, P., Krause, J. (2021). Early Cretaceous Mesochara-rich assemblages from central Patagonia, Argentina, predate the origin of homogenous Charoidean floras by about 30 million years. *Cretaceous Research*, 129: doi: 105017. 10.1016/j.cretres.2021.105017.
- De Sosa Tomas, A., Carignano, A., Vallati, P., and Martín-Closas, C. (2022). *Nuevos aportes al conocimiento micropaleontológico de la Formación Los Adobes (Grupo Chubut), Cretácico inferior, cuenca de Cañadón Asfalto*. XXI Congreso Geológico Argentino: poster, Puerto Madryn.
- D'Elía, L., Bilmes, A., Varela, A.N., Bucher, J., López, M., García, M., Ventura Santos, R., Hauser, N., Naipauer, M., and Franzese, J.R., (2020). Geochronology, sedimentology and paleosol analysis of a Miocene, synorogenic, volcanoclastic succession (La Pava Formation) in the north Patagonian foreland: Tectonic, volcanic and paleoclimatic implications. *Journal of South American Earth Sciences*, 100: doi.org/10.1016/j.jsames.2020.102555.
- Di Capua, A., and Scasso, R.A. (2020). Sedimentological and petrographic evolution of a fluvio-lacustrine environment

- during the onset of volcanism: Volcanically-induced forcing of sedimentation and environmental responses. *Sedimentology*, 67: 1879-1913.
- Echaurren, A., Folguera, A., Gianni, G., Orts, D., Tassara, A., Encinas, A., Giménez, M., and Valencia, V. (2016). Tectonic evolution of the North Patagonian Andes (41° - 44° S) through recognition of syntectonic strata. *Tectonophysics*, 677-678: 99-114.
- Edgett, K.S., and Lancaster, N. (1993). Volcaniclastic aeolian dunes: Terrestrial examples and application to martian sands. *Journal of Arid Environments*, 25: 271-297.
- Figari, E.G., and Hechem, J.J. (2022). Cuencas volcano-sedimentarias del Mesozoico. In: Giacosa, R.E. (Ed.): *Geología y Recursos Naturales de la Provincia del Chubut*. Relatorio del XXI Congreso Geológico Argentino: 129-141, Puerto Madryn.
- Figari, E.G., Scasso, R.A., Cúneo, R.N., and Escapa, I. (2015). Estratigrafía y evolución geológica de la Cuenca de Cañadón Asfalto, provincia del Chubut, Argentina. *Latin American Journal of Sedimentology and Basin Analysis*, 22: 135-169.
- Fisher, R.V. (1983). Flow transformations in sediment gravity flows. *Geology*, 11: 273-274.
- Fisher, J.A., Nichols, G.J., and Walthman, D.A. (2007). Unconfined flow deposits in distal sectors of fluvial distributary systems: examples from the Miocene Luna and Huesca systems, northern Spain. *Sedimentary Geology*, 195: 55-73.
- Foix, N., Allard, J.O., Paredes, J.M., and Giacosa, R.E. (2012). Fluvial styles, palaeohydrology and modern analogues of an exhumed, Cretaceous fluvial system: Cerro Barcino Formation, Cañadón Asfalto Basin, Argentina. *Cretaceous Research*, 34: 298-307.
- Foix, N., Allard, J.O., Ferreira, M.L., Atencio, M. (2020). Spatio-temporal variations in the Mesozoic sedimentary record, Golfo San Jorge Basin (Patagonia, Argentina): Andean vs. cratonic sources. *Journal of South American Earth Sciences*, 98: doi.org/10.1016/j.jsames.2019.102464.
- Galloway, W.E., and Hobday, D.K. (1996). *Terrigenous Clastic Depositional Systems: Applications to Fossil Fuel and Groundwater Resources*. Springer-Verlag, Nueva York, 491 pp.
- Gawthorpe, R.L. and Leeder, M.R. (2000). Tectono-sedimentary evolution of active extensional basins. *Basin Research*, 12: 195-218.
- Genise, J.F., Alonso-Zarza, A.M., Krause, J.M., Sánchez, M.V., Sarzetti, L., Farina, J.L., González, M.G., Cosarinsky, M., and Bellosi, E.S. (2010). Rhizolith balls from the Lower Cretaceous of Patagonia: just roots or the oldest evidence of insect agriculture? *Palaeogeography, Palaeoclimatology, Palaeoecology*, 287: 128-142.
- Georgieff, S.M., and Gonzalez Bonorino, G. (2002). Facies y geometrías de los depósitos aluviales cuaternarios en la quebrada del Portezuelo, sierra de Mojotoro, provincia de Salta, Argentina. *Revista de la Asociación Argentina de Sedimentología*, 9: 31-42.
- Giacosa, R.E. (2020). Basement control, sedimentary basin inception and early evolution of the Mesozoic basins in the Patagonian foreland. *Journal of South American Earth Sciences*, 97: doi.org/10.1016/j.jsames.2019.102407.
- Gianni, G., Navarrete, C., Orts, D., Tobal, J., Folguera, A., and Giménez, M. (2015). Patagonian broken foreland and related synorogenic rifting: the origin of Chubut Group Basin. *Tectonophysics*, 649: 81-99.
- Gianni, G.M., Likerman, J., Navarrete, C., Echaurren, A., Butler, K., and Folguera, A. (2022). *Antepais Fragmentado Patagónico: control estructural previo, mecanismos de deformación y sedimentación sintectónica*. In: Giacosa, R.E. (Ed.): *Geología y Recursos Naturales de la Provincia del Chubut*. Relatorio del XXI Congreso Geológico Argentino: 1293-1314, Puerto Madryn.
- Gibling, M.R. (2006). Width and thickness of fluvial channel bodies and valley fills in the geological record: a literature compilation and classification. *Journal of Sedimentary Research*, 76: 731-770.
- Glennie, K.W. (1987). Desert sedimentary environments, present and past. A summary. *Sedimentary Geology*, 50: 135-165.
- Hampton, B.A., and Horton, B.K. (2007). Sheetflow fluvial processes in a rapidly subsiding basin, Altiplano plateau, Bolivia. *Sedimentology*, 54: 1121-1147.
- Hauser, N., Cabaleri, N.G., Gallego, O.F., Monferran, M.D., Silva Nieto, D., Armella, C., Matteini, M., Aparicio González, P.A., Pimentel, M.M., Volkheimer, W., and Reimold, W.U. (2017). U-Pb and Lu-Hf zircon geochronology of the Cañadón Asfalto Basin, Chubut, Argentina: Implications for the magmatic evolution in central Patagonia. *Journal of South American Earth Sciences*, 78: 190-212.
- Hooper, D.M., McGinnis, R.N., and Necsoiu, M. (2012). Volcaniclastic aeolian deposits at Sunset Crater, Arizona: terrestrial analogs for Martian dune forms. *Earth Surface Processes and Landforms*, 37(10): 1090-1105.
- Houghton, B.F., Wilson, C.J.N., and Pyle, D.M. (2000). Pyroclastic fall deposits. In: Sigurdsson, H., Houghton, B.F., McNutt, S.R., Rymer, H., Stix, J. (Eds.), *Encyclopedia of Volcanoes*. Elsevier Academic Press: 555-570.
- Kataoka, K. (2023). From 'source to sink' to 'sink to source': a review of volcanic fluvial and lacustrine successions in Japan. In: Di Capua, A., De Rosa, R., Kereszturi, G., Le Pera, E., Rosi, M. and Watt, S. F. L. (Eds.), *Volcanic Processes in the Sedimentary Record: When Volcanoes Meet the Environment*. Geological Society, Special Publications, 520: 393 - 416.
- Kataoka, K., and Nakajo, T. (2002). Volcaniclastic re-sedimentation in distal fluvial basins induced by large-volume explosive volcanism: the Ebisutoge-Fukuda tephra, Plio-Pleistocene boundary, central Japan. *Sedimentology*, 49: 319-334.
- Kocurek, G. (1996). Desert eolian systems. In: Reading, H.G. (Ed.), *Sedimentary Environments, Processes, Facies and Stratigraphy*. Blackwell Science, Oxford: 125-153.
- Krause, J.M., Umazano, A.M., Bellosi, E.S., and White, T.S. (2014). *Hydromorphic paleosols in the upper Puesto La paloma Member, Cerro Barcino Formation, mid cretaceous, Patagonia Argentina: environmental and stratigraphic significance*. In: XIV Reunión Argentina de Sedimentología, 146-147. Puerto Madryn.
- Krause, J.M., Ramenazi, J., Umazano, A.M., Pol, D., Carballido, J.L., Sterli, J., Puerta, P., Cúneo, N.R., and Bellosi, E.S. (2020). High-resolution chronostratigraphy of the Cerro Barcino Formation (Patagonia): Paleobiologic implications for the mid-cretaceous dinosaur-rich fauna of South America. *Gondwana Research*, 80: 33-49.
- Lagorio, S., Busteros, A., Silva Nieto, D., Zaffarana, C., Giacosa, R., and González, P. (2022). El magmatismo Pérmico y Triásico de la región de Gastre y Sierra del Medio, suroeste del Macizo Norpatagónico. In: Giacosa,

- R.E. (Ed.): *Geología y Recursos Naturales de la Provincia del Chubut*. Relatorio del XXI Congreso Geológico Argentino: 291-329, Puerto Madryn.
- Langford, R.P. and Chan, M.A. (1989). Fluvial-eolian interactions: part II, ancient systems. *Sedimentology*, 36: 1037–1051.
- Lesta, P., and Ferello, R. (1972). Región extraandina de Chubut y norte de Santa Cruz. In: Leanza, A.F. (Ed.), *Geología Regional Argentina*. Academia Nacional de Ciencias Córdoba, Córdoba: 601-653.
- Manassero, M., Zalba, P.E., Andreis, R., and Morosi, M. (2000). Petrology of continental pyroclastic and epiclastic sequences in the Chubut Group (Cretaceous): Los Altares-Las Plumas area, Chubut, Patagonia Argentina. *Revista Geológica de Chile*, 27: 13-26.
- Manville, V., Németh, K., and Kano, K. (2009). Source to sink: a review of three decades of progress in the understanding of volcanoclastic processes, deposits and hazards. *Sedimentary Geology*, 220: 136-161.
- Martina, F., Dávila, F.M., and Astini, R.A. (2006). Mio-Pliocene volcanoclastic deposits in the Famatina Ranges, southern Central Andes: a case of volcanic controls on sedimentation in broken foreland basins. *Sedimentary Geology*, 186: 51-65.
- Melchor, R.N., Genise, J.F., Buatois, L., and Umazano, A.M. (2012). Fluvial environments. In: Knaust, D., Bromley, R.G. (Eds.), *Trace Fossils as Indicators of Sedimentary Environments*. Developments in Sedimentology, 64: 329-378.
- Melchor, R., Pérez, M., Villegas, P., Espinoza, N., Umazano, A., Cardonatto, M. (2023). Early Cretaceous lepidosaur (Sphenodontian?) burrows. *Scientific Reports*, 13, doi: 10.1038/s41598-023-37385-6.
- Miall, A.D. (1978). Facies types and vertical profile models in braided river deposits: a summary. In: Miall, A.D. (Ed.), *Fluvial Sedimentology*. Canadian Society of Petroleum Geologists Memoir, 5: 597-604.
- Miall, A.D. (1996). *The Geology of Fluvial Deposits: Sedimentary Facies, Basin Analysis and Petroleum Geology*. Springer-Verlag, Berlin, 582 pp.
- Miall, A.D. (2000). *Principles of Sedimentary Basin Analysis*. Springer-Verlag, Berlin, 616 pp.
- Miall, A.D. (2014). *Fluvial Depositional Systems*. Springer, Berlin, 316 pp.
- Monti, M., Franzese, J.R. (2016). Análisis tectonoestratigráfico del Grupo Puesto Viejo (San Rafael, Argentina): evolución de un rift continental triásico. *Latin American Journal of Sedimentology and Basin Analysis*, 23: 1-33.
- Moore, J.G., Peck, D.L. (1962). Accretionary lapilli in volcanic rocks of the western continental United States. *Journal of Geology*, 70: 182-193.
- Mountney, N.G. (2006). Eolian facies models. In: Posamentier, H.W., Walker, R.G. (Eds.), *Facies Models Revisited*. Society of Economic Paleontologists and Mineralogists Special Publication, 84: 19-83.
- Nakayama, C. (1973). *Sedimentitas prebayocianas en el extremo austral de la sierra de Taquetrén, Chubut, Argentina*. V Congreso Geológico Argentino: 269-278, Buenos Aires.
- Nakayama, K., and Yoshikawa, S. (1997). Depositional processes of primary to reworked volcanoclastics on an alluvial plain; an example from the Lower Pliocene Ohta tephra bed of the Tokai Group, central Japan. *Sedimentary Geology*, 107: 211-229.
- Nanson, G.C., and Croke, J.C. (1992). A genetic classification of floodplains. *Geomorphology*, 4: 459-486.
- Nichols, G.J., and Fisher, J.A. (2007). Processes, facies and architecture of fluvial distributary systems deposits. *Sedimentary Geology*, 195: 75-90.
- Paredes, J.M. (2022). *Sistemas Fluviales: Organización, Evolución e Importancia Económica*. Asociación Geológica Argentina, 602 pp.
- Paredes, J.M. (2023). Analogs in the study of fluvial successions: Conceptual framework and examples from the Chubut Group (Cretaceous) of Argentina. *Journal of South American Earth Sciences*, 123: doi.org/10.1016/j.jsames.2023.104202.
- Paredes, J.M., Foix, N., Colombo Piñol, F., Nillni, A., Allard, J.O., and Marquillas, R.A. (2007). Volcanic and climatic control on fluvial style in a high-energy system: the Lower Cretaceous Matasiente Formation, Golfo San Jorge Basin, Argentina. *Sedimentary Geology*, 202: 96-123.
- Paredes, J.M., Foix, N., Allard, J.O., Colombo, F., and Tunik, M.A. (2015). Alluvial architecture of reworked pyroclastic deposits in peri-volcanic basins: Castillo Formation (Albian) of the Golfo San Jorge Basin, Argentina. *Revista de la Asociación Geológica Argentina*, 72: 38-58.
- Paredes, J.M., Foix, N., Allard, J.O., Valle, M.N., and Giordano, S.R. (2018). Complex alluvial architecture, paleohydraulics and controls of a multichannel fluvial system: Bajo Barreal Formation (Upper Cretaceous) in the Cerro Ballena anticline, Golfo San Jorge Basin, Patagonia. *Journal of South American Earth Sciences*, 85: 168-190.
- Paredes, J.M., Giordano, S.R., Olazábal, S.X., Valle, M.N., Allard, J.O., Foix, N., and Tunik, M.A. (2020). Climatic control on stacking and connectivity of fluvial successions: Upper Cretaceous Bajo Barreal Formation of the Golfo San Jorge Basin, Patagonia. *Marine and Petroleum Geology*, 113: doi.org/10.1016/j.marpetgeo.2019.104116.
- Parrish, J.T. (1998). *Interpreting Pre-Quaternary Climate from the Geologic Record*. Columbia University Press, New York, 338 pp.
- Pérez, M., Umazano, A.M., and Visconti, G. (2013a). Análisis paleoambiental del Miembro Superior de la Formación Río Negro (Mioceno-Plioceno de Patagonia septentrional): un ejemplo de interacción fluvio-eólica compleja. *Revista de la Sociedad Geológica de España*, 26: 25-39.
- Pérez, M., Umazano, A.M., and Melchor, R.N. (2013b). *Cretaceous burrows of probable vertebrate origin from volcanoclastic interdune deposits of the Cerro Barcino Formation, Patagonia, Argentina*. II Latin American Symposium on Ichnology: 57, Santa Rosa.
- Pérez, M., Umazano, A.M., and Melchor, R.N. (2015). *Aeolian trace fossil associations from Cretaceous formations of Patagonia, Argentina: stratigraphic and ichnofacies implications*. III Latin American Symposium on Ichnology: 62, Colonia del Sacramento.
- Petrinovic, I.A., and D'Elía, L. (2018). *Rocas Volcanoclasticas. Depósitos, Procesos y Modelos de Facies*. Asociación Argentina de Sedimentología, La Plata, 172 pp.
- Pierson, T.C., and Major, J.J. (2014). Hydrogeomorphic effects of explosive volcanic eruptions on drainage basins. *Annual Review of Earth and Planetary Sciences*, 42: 469-507.
- Platt, N.H. and Keller B. (1992). Distal alluvial deposits in a foreland basin setting—the Lower Freshwater Molasse (Lower Miocene), Switzerland: sedimentology, architecture and palaeosols. *Sedimentology*, 39: 545–565.
- Pol, D., Garrido, A., and Cerda, I.A. (2011). A New Sauropodomorph Dinosaur from the Early Jurassic of

- Patagonia and the Origin and Evolution of the Sauropod-type Sacrum. *PLoS ONE*, 6: doi.org/10.1371/journal.pone.0014572.
- Proserpio, C.A. (1987). *Hoja Geológica 44 e, Valle General Racedo, Provincia de Chubut*. Dirección Nacional de Minería y Geología, Secretaría de Minería, scale 1:200000.
- Pye, K., and Tsoar, H. (2009). *Aeolian Sand and Sand Dunes*. Springer, Berlin, 458 pp.
- Raigemborn, M.S., Matheos, S.D., Krapovickas, V., Vizcaíno, S.F., Bargo, M.S., Kay, R.F., Fernicola, J.C., and Zapata, L. (2015). Paleoenvironmental reconstruction of the coastal Monte León and Santa Cruz formations (Early Miocene) at Rincón del Buque, Southern Patagonia: A revisited locality. *Journal of South American Earth Sciences* 60: 31-55.
- Raigemborn, M.S., Beilinson, E., Krause, J.M., Varela, A.N., Bellosi, E.S., Matheos, S.D., and Sosa, N. (2018). Paleolandscape reconstruction and interplay of controlling factors of an Eocene pedogenically-modified distal volcaniclastic succession in Patagonia. *Journal of South American Earth Sciences*, 86: 475-496.
- Schumacher, R., Schmincke, H.U. (1995). Model for the origin of accretionary lapilli. *Bulletin of Volcanology*, 56: 626-639.
- Sierra, S., Moreno, C., and Pascual, E. (2009). Stratigraphy, petrography and dispersion of the Lower Permian syn-eruptive deposits in the Viar Basin, Spain. *Sedimentary Geology*, 217: 1-29.
- Smith, G.A. (1991). Facies sequences and geometries in continental volcaniclastic sediments. In: Fisher, R.V., Smith, G.A. (Eds.), *Sedimentation in Volcanic Settings*. Society of Economic Paleontologists and Mineralogists, Special Publication, 45: 109-121.
- Smith, G. A. and Katzman, D. (1991). Discrimination of eolian and pyroclastic surge processes in the generation of crossbedded tuffs, Jemez Mountains volcanic field, New Mexico. *Geology*, 19(5): 465-468.
- Smith, G.A. and Lowe, D.R. (1991). Lahars: volcano-hydrologic events and deposition in the debris flow-hyperconcentrated flow continuum. In: Fisher, R.V., Smith, G.A. (Eds.), *Sedimentation in Volcanic Settings*. Society of Economic Paleontologists and Mineralogists, Special Publication, 45: 59-70.
- Smith, A.G., Hurler, A.M. y Briden, J.C. (1981). *Phanerozoic Paleontological World Maps*. Cambridge University Press, Cambridge, 102 pp.
- Smoot, J.P. and Lowenstein, T.K. (1991). Depositional environments of non-marine evaporites. In: Melvin, J.L. (Ed.), *Evaporites, Petroleum and Mineral Resources*. Developments in Sedimentology, 50: 189-347.
- Sohn, Y.K., Ki, J.S., Jung, S., Kim, M., Cho, H., and Son, M. (2013). Synvolcanic and syntectonic sedimentation of the mixed volcaniclastic-epiclastic succession in the Miocene Janggi Basin, SE Korea. *Sedimentary Geology*, 288: 40-59.
- Spalletti, L.A., and Colombo Piñol, F. (2019). Architecture of interuptive and syneruptive facies in an Andean quaternary palaeovalley: The huarenchenque formation, western Argentina. *Andean Geology*, 46: 471-489.
- Sterli, J., de la Fuente, M.S., and Umazano, A.M. (2015). New remains and new insights on the Gondwanan meiolaniform turtle *Chubutemys copelloi* from the Lower Cretaceous of Patagonia, Argentina. *Gondwana Research*, 27: 978-994.
- Stipanovic, P.N., Rodrigo, F., Baulies, O., and Martínez, C. (1968). Las formaciones presenonianas en el denominado Macizo Norpatagónico y regiones adyacentes. *Revista de la Asociación Geológica Argentina*, 23: 67-98.
- Talbot, M.R., and Allen, P.A. (1996). Lakes. In: Reading, H.G. (Ed.), *Sedimentary Environments: Processes, Facies and Stratigraphy*. Blackwell Science, Cambridge: 83-124.
- Uliana, M.A., and Biddle, K.T. (1987). Permian to late Cenozoic evolution of northern Patagonia: main tectonic events, magmatic activity, and depositional trends. *American Geophysical Union Memoir*, 40: 271-286.
- Umazano, A.M., Bellosi, E.S., Visconti, G., and Melchor, R.N. (2008). Mechanisms of aggradation in fluvial systems influenced by explosive volcanism: an example from the Upper Cretaceous Bajo Barreal Formation, San Jorge Basin, Argentina. *Sedimentary Geology*, 203: 213-228.
- Umazano, A.M., Bellosi, E.S., Visconti, G., and Melchor, R.N. (2012). Detecting allocyclic signals in volcaniclastic fluvial successions: facies, architecture and stacking pattern from the Cretaceous of central Patagonia, Argentina. *Journal of South American Earth Sciences*, 40: 94-115.
- Umazano, A.M., Melchor, R.N., Bedatou, E., Bellosi, E.S., and Krause, J.M. (2014). Fluvial response to sudden input of pyroclastic sediments during the 2008-2009 eruption of the Chaitén volcano (Chile): the role of logjams. *Journal of South American Earth Sciences*, 54: 140-157.
- Umazano, A.M., Krause, J.M., Bellosi, E.S., Pérez, M., Visconti, M., and Melchor, R.N. (2017). Changing fluvial styles in volcaniclastic successions: a cretaceous example from the Cerro Barcino Formation, Patagonia. *Journal of South American Earth Sciences*, 77: 185-205.
- Umazano, A.M., and Melchor, R.N. (2020). Volcaniclastic sedimentation influenced by logjam breakups? An example from the Blanco River, Chile. *Journal of South American Earth Sciences*, 98: doi.org/10.1016/j.jsames.2019.102477.
- Umazano, A.M., Melchor, R.N., Bedatou, E., and Krause, J.M. (2021). *Improving the facies models for syn-eruptive fluvial successions: lessons from the Chaitén volcano and Blanco river, Chile*. XVII Reunión Argentina de Sedimentología and VIII Congreso Latinoamericano de Sedimentología: Actas, Paraná.
- Umazano, A.M., Bedatou, E., Krause, J.M., Bellosi, E.S., and Villegas, P. M. (2022). Improving the facies model for syn-eruptive fluvial successions: lessons from the Chaitén volcano and Blanco river, Chile. *Latin American Journal of Sedimentology and Basin Analysis*, 29: 61 - 65.
- Villegas, P.M. (2022). *Rol de los Factores Alocíclicos en la Sedimentación de Sucesiones Fluviales Volcanoclásticas: el Caso de la Formación Cerro Barcino, Cretácico de Patagonia*. Tesis Doctoral, Facultad de Ciencias Físico-Matemáticas y Naturales, Universidad Nacional de San Luis, 285 pp. (inédito).
- Villegas, P.M., Visconti, G., and Umazano, A.M. (2014). *Respuestas sedimentarias de un sistema fluvial al influjo de sedimentos piroclásticos: el caso de los miembros Bardas Coloradas y Puesto La Paloma durante el Cretácico de Patagonia*. XIV Reunión Argentina de Sedimentología: 295-296, Puerto Madryn.
- Villegas, P.M., Umazano, A.M., Melchor, R.N., and Kataoka, K. (2019). Soft-sediment deformation structures in gravelly fluvial deposits: A record of Cretaceous seismic activity in Patagonia? *Journal of South American Earth Sciences*, 90: 325-337.
- Volkheimer, W., Gallego, O.F., Cabaleri, N.G., Armella, C., Narváez, P.L., Silva Nieto, D.G., and Páez, M.A. (2009).

- Stratigraphy, palynology and conchostracans of a Lower Cretaceous sequence at the Cañadón Calcáreo locality, extra-andean central Patagonia: age and paleoenvironmental significance. *Cretaceous Research*, 30: 270-282.
- Walker, G.P.L. (1973). *Explosive volcanic eruptions: a new classification scheme*. *Geologische Rundschau*, 62: 431-446.
- Westoby, M., Brasington, J., Glasser, N., Hambrey, M. and Reynolds, J. (2012). 'Structure-from-Motion' photogrammetry: A low-cost, effective tool for geoscience applications. *Geomorphology*, 179: 300-314.
- White, J. D. L. (1989). Basic elements of maar-crater deposits in the Hopi Buttes volcanic field, northeastern Arizona, U.S.A. *Journal of Geology*, 97(1): 117-125.
- White, J. D. L. (1990). Depositional architecture of a maar-pitted playa: Sedimentation in the Hopi Buttes volcanic field, northeastern Arizona, U.S.A. *Sedimentary Geology*, 67: 55-84.